THE CALCULATION OF AXIS REACTANCES OF RELUCTANCE MOTORS WITH AXIALLY LAMINATED, MAGNETICALLY ANISOTROPIC ROTORS

A Thesis

Submitted to the Faculty of Graduate Studies

in Partial Fulfillment of the Requirements for the

Degree of Master of Science

Department of Electrical Engineering

The University of Manitoba

Winnipeg, Canada.

by

H.W. LEE

MAY 1971

ABSTRACT

A numerical approach considering a magnetic circuit is developed to calculate the axis reactances of a reluctance motor with an axially laminated, magnetically anisotropic rotor. The rotor is divided into a large number of sections with each containing more than one lamination. In each section, there is a magnetomotive force acting across the permeance of the air gap and the reluctance of the laminations. A lattice network is thus formed. For a study of saturation, the non-linear permeance of the stator teeth is considered using the single valued B-H characteristic of the stator iron. A space factor relating the effective cross-sectional area of the teeth to the actual area of the section is introduced to modify the B-H characteristics. The combination of the permeance of the air gap and the stator teeth gives the effective permeance of the air gap. Using superposition, the air gap flux density distribution for each section is calculated. (Iteration is used when considering saturation as the permeance of the stator teeth changes and the magnetomotive force across the air gap varies.) The axis reactances are calculated from a knowledge of the flux density distribution.

ACKNOWLEDGEMENT

The author wishes to express his deepest gratitude to all those who have assisted in any way. The University of Manitoba's Electrical Engineering Faculty for the facilities and National Research Council for financial support of the project. A special thanks to Dr. R.M. Mathur and Dr. R.W. Menzies for their keen interest and assistance.

TABLE OF CONTENTS

LIST OF ILLUSTRATIONS

LIST OF SYMBOLS

A	- area	m^2
B	- flux density	T
C	- coefficient of Fourier Series	
F	- amplitude of magnetomotive force	A
H	- magnetic field potential	A/m
H	- element of permeance matrix	Wb/A
I	- current	A
K_1	- first harmonic winding factor	
K_d	- ratio of direct-axis magnetising reactance to cylindrical magnetising reactance	
M	- numbers of phase in stator	
MMF	- magnetomotive force	A
N	- dummy variable	
N	- subscript: N-th component	
P	- permeance	Wb/A
P	- average power	W
R	- reluctance	A/Wb
R_a	- resistance of phase a winding	Ω
S	- space factor	
T	- torque	N.m.
V	- voltage	V
X	- reactance	Ω
Z	- impedance	Ω

(List of Symbols - continued)

a	- subscript: phase a	
b	- coefficient constant of Fourier series	
c	- subscript: cylindrical	
d	- subscript: direct-axis	
g	- radial air gap length	m
i	- subscript: iron	
l	- subscript: leakage	
l	- axial length of rotor	m
mc	- subscript: cylindrical magnetising	
md	- subscript: direct-axis magnetising	
ms	- subscript: stator magnetising	
n	- numbers of sections	
n	- numbers of turns/pole/phase	
n.l.	- subscript: no load	
o	- subscript: air	
o	- subscript: loss	
p	- number of stator pole-pair	
q	- subscript: quadrature-axis	
r	- radius of rotor	m
s	- stacking factor	
s	- subscript: stator	
ω	- angular velocity in radian	

(List of Symbols - continued)

β	- angular position in radian of rotor's quadrature axis measured from a reference axis	
Φ	- flux	Wb
ε	- angle subtended by each section	
λ	- flux linkage	Wb
θ	- angular distance in radian, measured around the air gap from a ref. axis	
μ	- permeability	N/A^2
ρ	- inner limit of laminations in radian measured from quadrature-axis	
σ	- outer limit of laminations in radian measured from quadrature-axis	
δ_e	- load angle using voltage as reference	
δ_i	- load angle using current as reference	
γ	- angular distance in radian from the rotor quadrature-axis to a specific lamination	

CHAPTER I

INTRODUCTION

The reluctance motor is a synchronous machine; i.e. a machine which turns at a speed dependent on the frequency of the alternating voltage supplied and the number of pole-pair in the machine. The rotor of the machine is characterized by offering low reluctance - or resistance to the establishment of magnetic flux along one axis and high reluctance along the other at 90 electrical degrees to the first. The principle of operation is that torque is developed as the stator MMF aligns or tends to align the rotor in a position where the establishment of magnetic flux is easiest. A common type of reluctance motor is the salient-pole rotor type. A simple illustration showing a 4-pole, salient-pole motor is in Figure 1(a). The synchronous performance of the motor, such as power factor, torque and efficiency, depends largely on the difference in reluctance along the two axes in the rotor. The rotor requires no electrical contact. Hence it is also simple and can be constructed in a reliable and robust fashion. The simplicity of construction makes it a relatively inexpensive machine.

Therefore, due to the simple and reliable construction, and the characteristics of speed and position of the rotor fixed by the frequency of the supply, the reluctance motor is employed in driving highly sophisticated systems.

An example is the high quality sound and picture reproducing equipment. In the case of digital computer data store, the write and pick up heads are controlled by pneumatic means. The operation of these heads are synchronized precisely with the movement of the discs. Both operations are under the control of a single reluctance motor.

Reluctance motors can also be caused to run in exact synchronisation with each other. The control system is relatively simple as there is no need to monitor the speed or position achieved by the motor and to feed this back for comparison with some demanded values. The control properties (i.e. speed and position) can be exploited in an open-loop situation. The practical value of this is enormous. An example is in machinery for spinning and winding chemical textiles. Liquid textile is pumped at a controlled rate through spinnerettes, forming filaments of fibre and then passing them over driven rollers through special chambers where their physical conditions are stabilised and then wound onto bobbins. The whole operation, pumping, stabilisation and winding, involved the use of separate motors, all of which must be precisely controlled and synchronised with respect to each other. Otherwise, the filament thickness would vary continuously resulting in poor quality of the product, if not in breakage of the filament[1].

Many other applications in connection with turning

operations can be mentioned; however, the reluctance motor has not been desirable in the large field of single drive systems or conveyor systems. This is because of poor power factor, usually about 0.4 and low efficiency, at most 50%. It is necessary to note that these qualities were attributed to poor rotor design. Shown in Figure 1(a) is the early type rotor designed with low pole-span to pole-pitch ratio. This meant a relatively stronger stator MMF was required to establish magnetic flux across the air gap because of greater reluctance. Large magnetising current was required. This large flow of current resulted in heavy copper loss and hence low efficiency. The ratio of the reactances of the two axis was also lower because of the large air gap and so gave poor power factor. Kostko in 1923 proposed a design to increase the pole-span to pole-pitch ratio and to decrease the air gap length. He also realized that not only external magnetic dissymmetry might be controlled but that the internal magnetic anisotropy of the rotor was of equal importance[2]. Shown in Figure 1(b) the proposal included flux guides or flux barriers for better internal magnetic anisotropy of the rotor. Further development was carried by Risch[3] as demand for better performance in reluctance motors increased. Figure 1(c) shows Risch's design which was commercially available in 1956. The design shows similar features to Kostko. The present type rotor, shown in Figure 1(e) was a modification of the early type rotor. The modifications were the features proposed by Kostko and others. The rotor is still commercially available

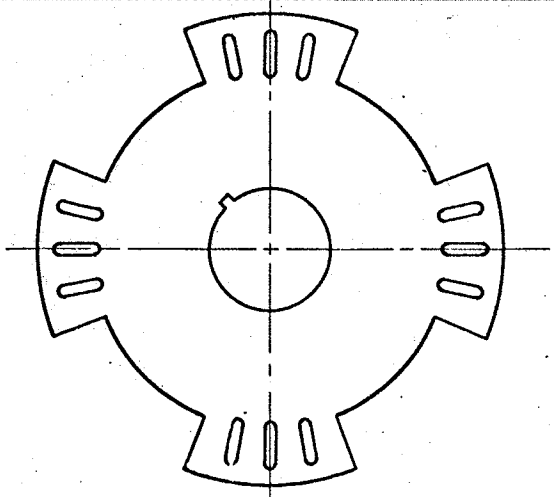

a. EARLY TYPE

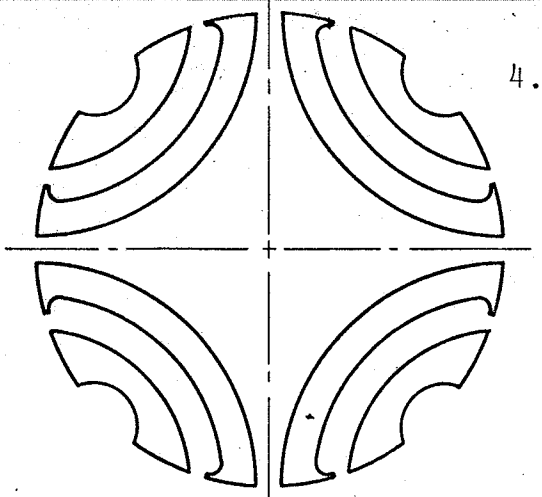

b. KOSTKO 1923

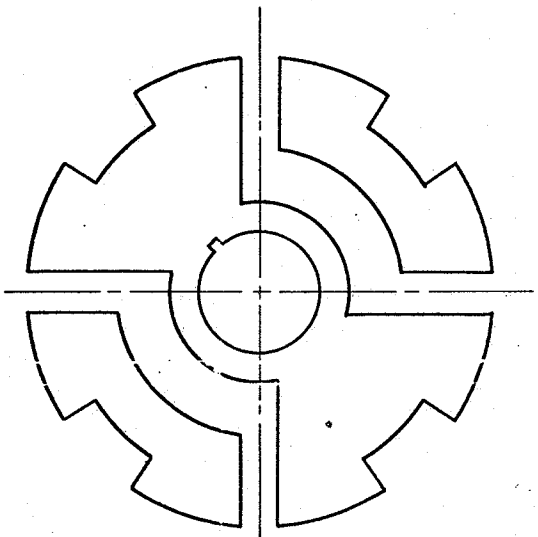

c. RISCH 1956

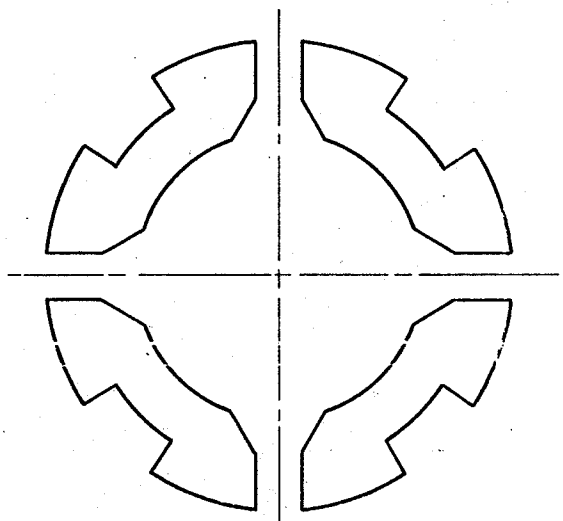

d. LAWRENSON 1965

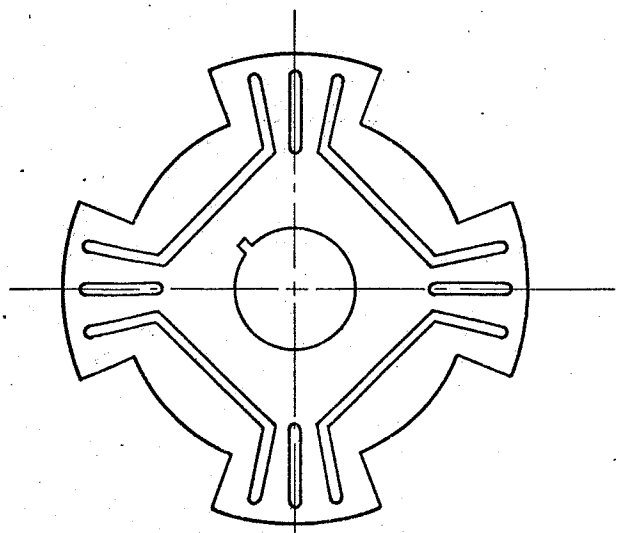

e. PRESENT TYPE

FIGURE 1: DEVELOPMENT OF RELUCTANCE MOTORS

along with other later designs. The reluctance motor was further developed, not only for better synchronous performances but for asynchronous performance as well. For example, the motor was designed to have: lower starting current, ability to start from rest, and better synchronising ability. Figure 1(d) shows Lawrenson's segmental rotor design in 1965. This design is now commercially manufactured in Britain.

The construction of the earlier and present type rotor, shown in Figure 1(a) and 1(e) could be easily visualised as a circular lamination of steel stamped into the external shape of the rotor and the cut-outs of the rotor. It was then stacked and mounted with magnetic insulation along the length of the rotor shaft. The air gaps and the cut-outs were filled with aluminium which has the permeance of air, and the rotor was then machined down to a cylindrical shape. In the case of the segmental rotor as shown in Figure 1(d), the process was not too difficult from the above process. A slightly larger diameter than that of the rotor lamination was stamped. The disc was then stamped into the internal shape of the rotor. The four segments were attached in their appropriate positions to the ring which was the extra radius of the disc. Laminae were then stacked and mounted onto a shaft. The rotor was die cast with aluminium. The outer ring was machined off giving the rotor the proper diameter. The segments have been modified from that as shown in Figure 1(d). A dove tail was provided on the inside of the segments

into which aluminium was filled. The aluminium would then hold the segments in place against the pull of the centrifugal force during the rotation of the rotor.

In an attempt to produce higher reactance ratios, the orthodox method of stamping and stacking rotor laminations on a shaft was abandoned and an axially laminated, magnetically anisotropic rotor was developed[4]. The magnetically anisotropic steel has a higher permeance or lower reluctance along the direction of rolling than in the two perpendicular directions. The magnetic insulation between laminations also serves to increase the reluctance in the two perpendicular directions. If the steel was wound or bent into a C-shape and installed onto a shaft as shown in Figure 2, this would give external magnetic dissymetry as well as the internal magnetic anisotropy. The construction of the rotor was extremely simple. A strip of cold-rolled grain-oriented steel was wound on a circular form by the standard C-core winding technique. It was cut into quadrants, assembled onto a shaft and machined to a circular form.

The analysis of the reluctance motor has been developed in two ways. The first was by the adaption of the results for salient-pole synchronous machine, as developed by Park[5], Doherty and Nickle[6], by putting all the excitation terms to zero. The second was developed from first principles. The idea was to take the air gap permeance and the MMF acting across the gap and determine from them, the flux density distribution in the air gap. This method was longer but would

FIGURE 2: 4 POLE, AXIALLY LAMINATED MAGNETICALLY ANISOTROPIC ROTOR

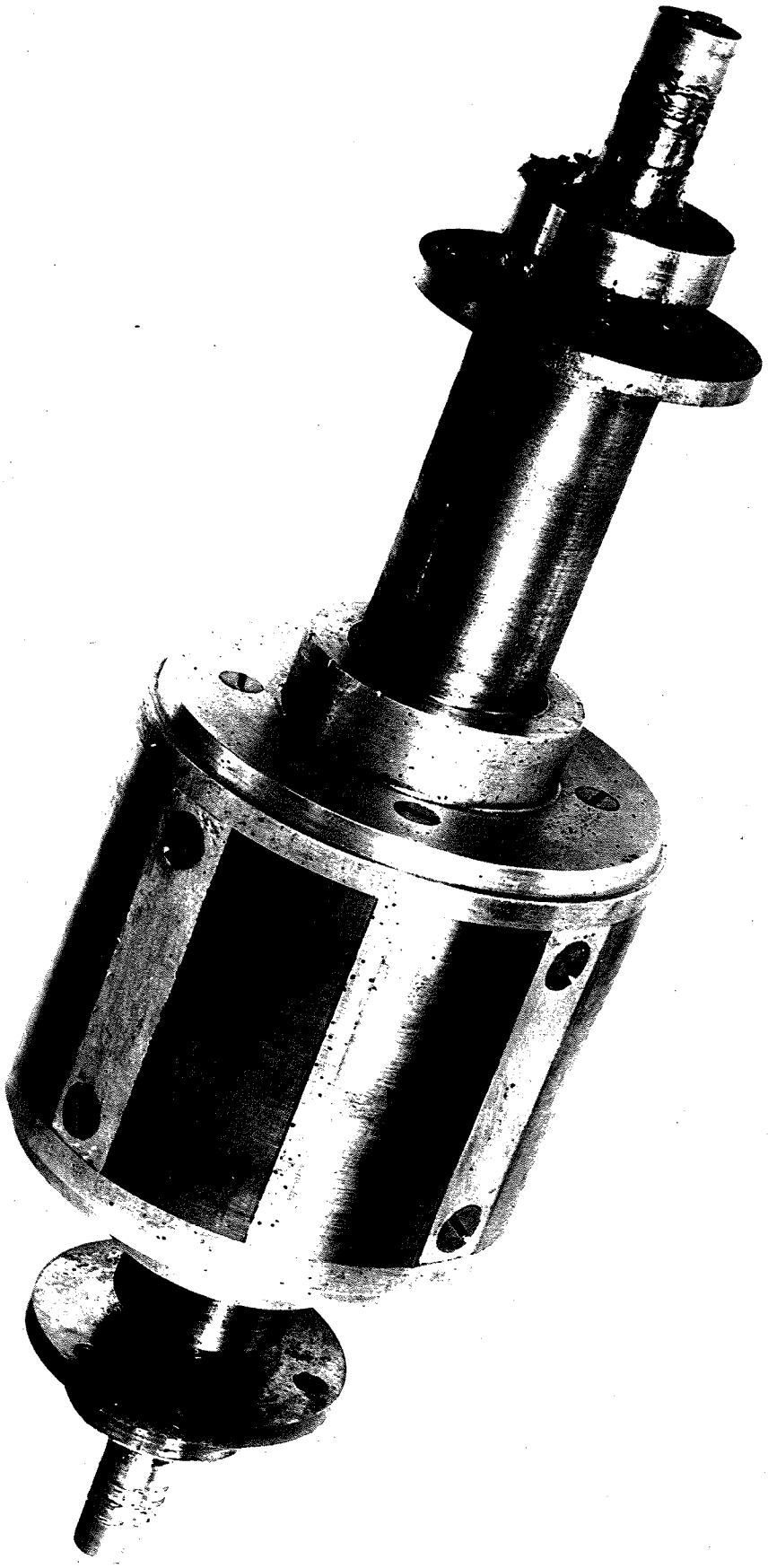

give a clearer picture because of its first principle approach rather than an adaptation of some other results. Both approaches were based on the two-axis theory which assumed the variation of the MMF in the air gap to be a second harmonic function. The approach also required the axis reactances be expressed in terms of machine dimensions. From the axis reactances, the synchronous characteristics of the motor such as power factor and torque were calculated.

The conventional approach in the analysis of the reluctance motor with the earlier type rotor assumed an infinite permeability of the rotor and zero rotor magnetic potential. The modern designs, characterised by flux guides, flux channels and also the use of anisotropic materials, resulted in analytical complexities, most of which arose on account of a magnetic potential developed in the rotor.

In the "Theory and Performance of Polyphase Reluctance Machines"[7], Lawrenson presented a method of analysis based on the second approach. Applying the analysis to a new form of rotor, he pointed out the presence of flux reversal in the air gap which he associated with the condition that the rotor takes on a magnetic potential other than zero. He argued that in a typical pole, the rotor potential was equal to the stator potential at the point of flux reversal which can be determined by using the fact that flux does not accumulate in the pole. Summing all the flux leaving or entering the pole-face, he equated it to the flux leaving the sides of

the pole and the point of flux reversal was determined. The rotor potential was then assumed to be a square wave function with a width of the pole-span. The fundamental component of the rotor potential was then evaluated using Fourier series analysis. This sinusoidal term was then used in the calculation of the air gap flux density distribution. This method worked well for his design but he indicated that in the case of small pole-span, the fundamental component of the rotor potential would tend to zero. But at the point of flux reversal, the rotor potential must approach the value of the stator potential. As the stator potential was unlikely to be near zero, the result was unacceptable. This method then, did not deal adequately with the problem of rotor potential. It also did not deal with the problem of saturation in the motor without introducing mathematics of a high degree of complexity and sophistication, which might not be justifiable in terms of time and cost.

The complexities introduced by the axially laminated anistropic rotor proved too difficult for analytical methods used previously without introducing simplifying assumptions. To overcome this impass, a numerical approach was developed which dealt more adequately with the problem of rotor potential anisotropy and saturation. The program was simple and unlike the finite difference method[8], did not involve complicated considerations such as boundary conditions in order to calculate the magnetic flux distribution in the air gap. It was

sufficiently general and could be easily handled by computer. It allowed for, as in Lawrenson's method, the consideration of design parameters such as pole-span to pole-pitch ratio, primary circuit impedance and the number of pole-pairs. It also allowed for consideration of the degree of anisotropy and stacking factor, parameters unique to the axially laminated, anisotropic rotor.

In the first chapter, the analysis of the polyphase machine leads to the calculation of axis reactances. The second deals with the numerical approach as applied to an axially laminated, magnetically anisotropic rotor. The third chapter handles the problem of saturation and the iterative methods involved. The fourth chapter compares the calculated values of axis reactances with the experimental values of a test machine. Predicted synchronous performances of torque and power factor are also compared with experimental values in that chapter.

1. ANALYSIS OF POLYPHASE MACHINE

Papers on the analysis of the polyphase machine are abundant[9]. Rather than repeating the rigorous mathematics involved, a brief qualitative analysis is given here. In Figure 3, a 4-pole axially laminated magnetically anisotropic rotor is shown.

Assume a sinusoidal current distribution in the stator winding; the stator MMF is then given as

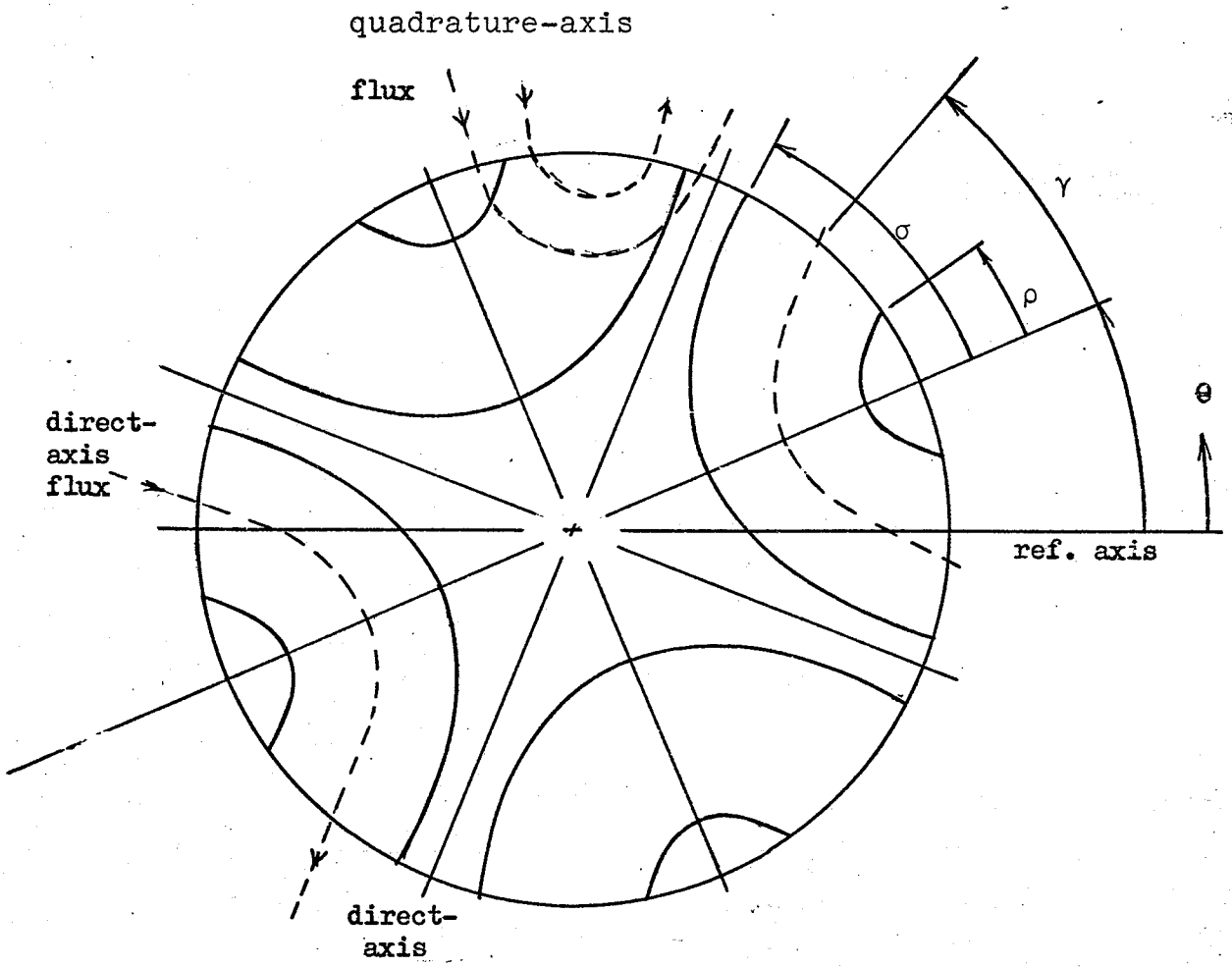

FIGURE 3: 4-POLE, AXIALLY LAMINATED MAGNETICALLY ANISOTROPIC ROTOR: MAGNETIC CIRCUIT

$$\underline{F} = \frac{2\ M_s\ K_1\ n\underline{I}}{\pi} \qquad \ldots(1)$$

where $\underline{F}$ and $\underline{I}$ are the RMS amplitudes of the MMF and current respectively. The flux density in the air gap is then

$$\underline{B} = \frac{\mu_o\ \underline{F}}{g} \qquad \ldots(2)$$

where $\underline{B}$ is the RMS amplitude of the flux density.

For a cylindrical rotor, the flux density distribution would be sinusoidal; however, as the pole-span decreases this is no longer so. The distribution is then expressed as a Fourier series.

$$\sin\ \theta = \sum_{N=1}^{\infty} b_N\ \sin\ N\theta \qquad \ldots(3)$$

where θ is the angular distance measured around the air gap in electrical radians from a reference axis.

As MMF is assumed to be purely fundamental, there is flux linkage for the fundamental component of flux density only.

$$\lambda = 2\ p\ n\ K_1 \int_o^{\pi/p} B_\theta\ l\ r\ d\theta \qquad \ldots(4)$$

where B_θ is the flux density function represented by the fundamental component only. The rate of change of the flux linkage is the induced voltage. In the direct-axis position,

$$V_{ms} = j\ X_{md}\ I_{ms} \qquad \ldots(5)$$

The coefficient of the fundamental component b_1 in B_θ, shows up in the reactance term.

$$X_{md} = \frac{24\ \mu_o\ (n\ K_1)^2\ \omega\ l\ r\ b_1}{\pi g} \qquad \ldots(6)$$

In the case of a cylindrical rotor, the coefficient b_1 is equal to unity. The magnetising reactance of the cylindrical rotor is

$$X_{mc} = \frac{24\ \mu_o\ (n\ K_1)^2\ \omega\ l\ r}{\pi g} \qquad ...(7)$$

If the ratio of the amplitudes of the fundamental component of the flux density in the direct-axis position to that of the cylindrical rotor is known, then this ratio K_d would give the direct-axis magnetising reactance.

$$X_{md} = K_d\ X_{mc} \qquad ...(8)$$

The direct-axis reactance is then

$$X_d = X_{md} + X_l \qquad ...(9)$$

where X_l is the leakage reacatance. The quadrature-axis reactance is similarly derived.

2. SYNCHRONOUS OPERATION

If the RMS terminal voltage is V_a (phase voltage), and the RMS terminal current is I_a (current in phase a), then in the two-axis transformed model, as shown in Figure 4

$$V_d = -\ V_a \sin \delta_e$$
$$V_q = \quad V_a \cos \delta_e \qquad ...(10)$$

From two-axis theory

$$V_d = R_a\ I_d - X_q\ I_q$$
$$V_q = R_a\ I_q + X_d\ I_d \qquad ...(11)$$

From this system of equations, I_d and I_q can be solved[10].

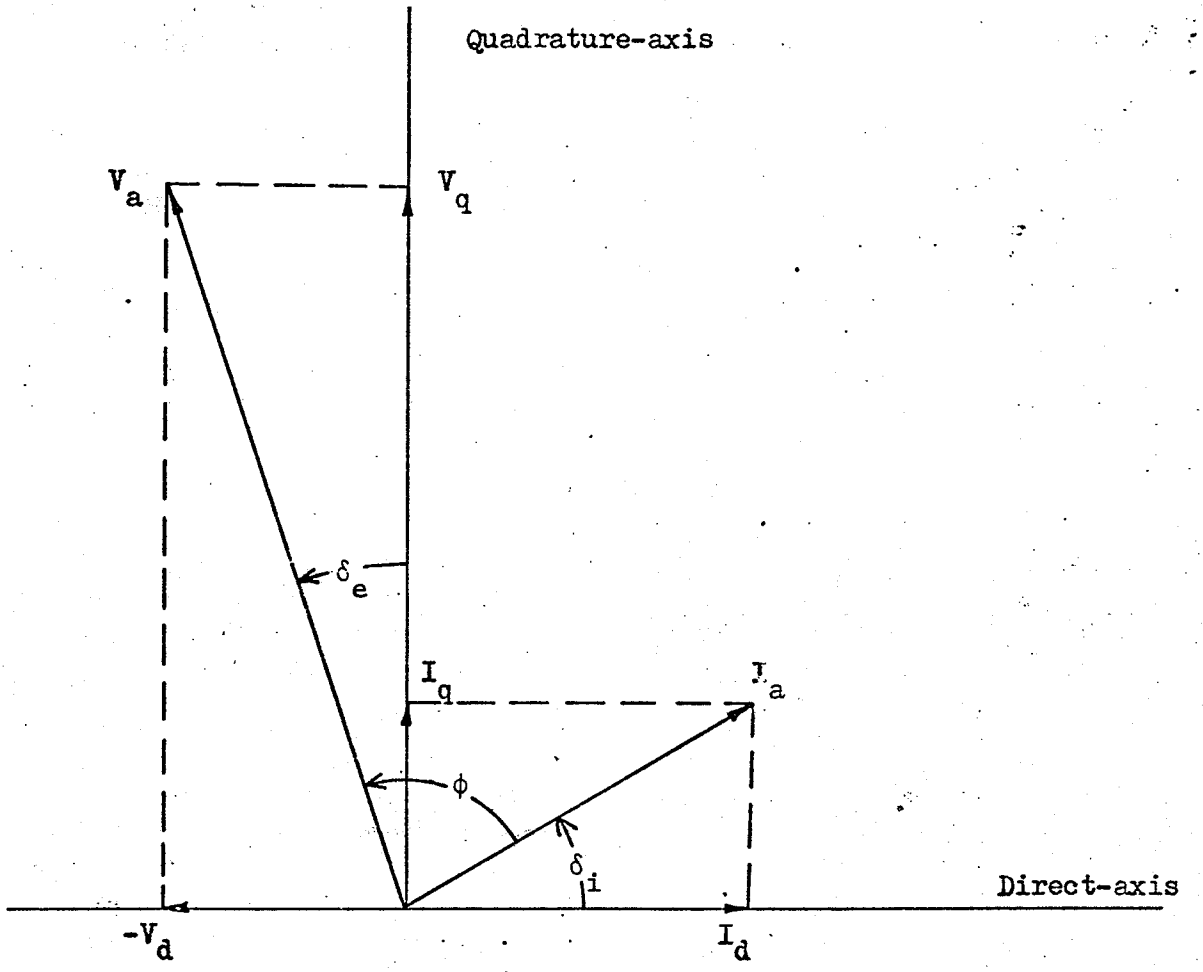

FIGURE 4: PHASOR DIAGRAM OF TERMINAL VOLTAGE AND CURRENT

Combining equations (10) and (11)

$$I_d = \frac{V_a \cos \delta_e \cdot X_q - V_a \sin \delta_e \cdot R_a}{R_a^2 + X_d X_q} \qquad ...(12)$$

$$I_q = \frac{V_a \cos \delta_e \cdot R_a + V_a \sin \delta_e \cdot X_d}{R_a^2 + X_d X_q} \qquad ...(13)$$

Let the iron loss per phase of the motor be P_o and as iron loss is proportional to the square of the terminal voltage,

$$P_o = \frac{V_a^2}{R_o} \qquad ...(14)$$

where R_o is the iron loss resistance which is placed across the terminal. Therefore the loss current component, I_o, is given as

$$I_o = \frac{V_a}{R_o} \qquad ...(15)$$

and is in phase with the terminal voltage V_a. Hence the modified terminal current, I_a' is

$$I_d' = I_d - I_o \sin \delta_e$$

$$I_q' = I_q - I_o \cos \delta_e$$

$$I_a' = (I_d'^2 + I_q'^2)^{1/2} \qquad ...(16)$$

From Figure 4, the power factor angle can be determined as

$$\phi = \delta_e + \tan^{-1} \left(\frac{I_d'}{I_q'}\right) \qquad ...(17)$$

If the total average power of the motor is P_T, then

$$P_T = 3\ (V_d\ I'_d + V_q\ I'_q) \qquad \ldots(18)$$

From equations (11) and (16)

$$P_T = 3\ R_a\ I'^{2}_a + 3\ (X_d - X_q)\ I'_d\ I'_q \qquad \ldots(19)$$

It is evident that the first term represents copper loss, and the second term the iron loss and the air gap power. Hence the air gap power P_m is

$$P_m = 3\ (X_d - X_q)\ I_q\ I_d \qquad \ldots(20)$$

From equation (20), it is possible to calculate the shaft torque developed by the machine, provided that the windage loss is taken into consideration.

From equation (1) to (9), the axis reactances can be calculated and from equation (10) to (20), the synchronous performance of the machine can be predicted.

CHAPTER II

THE MAGNETIC EQUIVALENT CIRCUIT

The rotor of the reluctance motor was divided into n-sections. If we considered a section of the rotor (see Figure 5), e.g. the i-th section, there would be a magnetomotive force F(i) acting across the iron in the stator teeth of permeance $P_i(i)$ and the air gap of permeance $P_o(i)$. Relucatance R(i) due to anisotropy and insulation between the i-th and the (i-1)-th sections formed the leg of the lattice equivalent circuit as shown in Figure 6. The iron and air permeance were combined into one permeance P(i)

$$P(i) = \frac{P_i(i)\ P_o(i)}{P_i(i)+P_o(i)} \qquad \ldots(21)$$

1. THE PERMEANCE MATRIX

Calculation of the permeance matrix was based on superposition. The flux of each leg of the lattice network was worked out for each stator magnetomotive force with all other forces shorted. For the i-th section, the reluctance to the left of the section of the lattice was $R_n(i)$ where

$$R_n(i) = R(i) + \frac{1}{P(i-1) + \frac{1}{R_n(i-1)}} \qquad \ldots(22)$$

and to the right was $R_p(i)$ where

$$R_p(i) = R(i+1) + \frac{1}{P(i+1) + \frac{1}{R_p(i+1)}} \qquad \ldots(23)$$

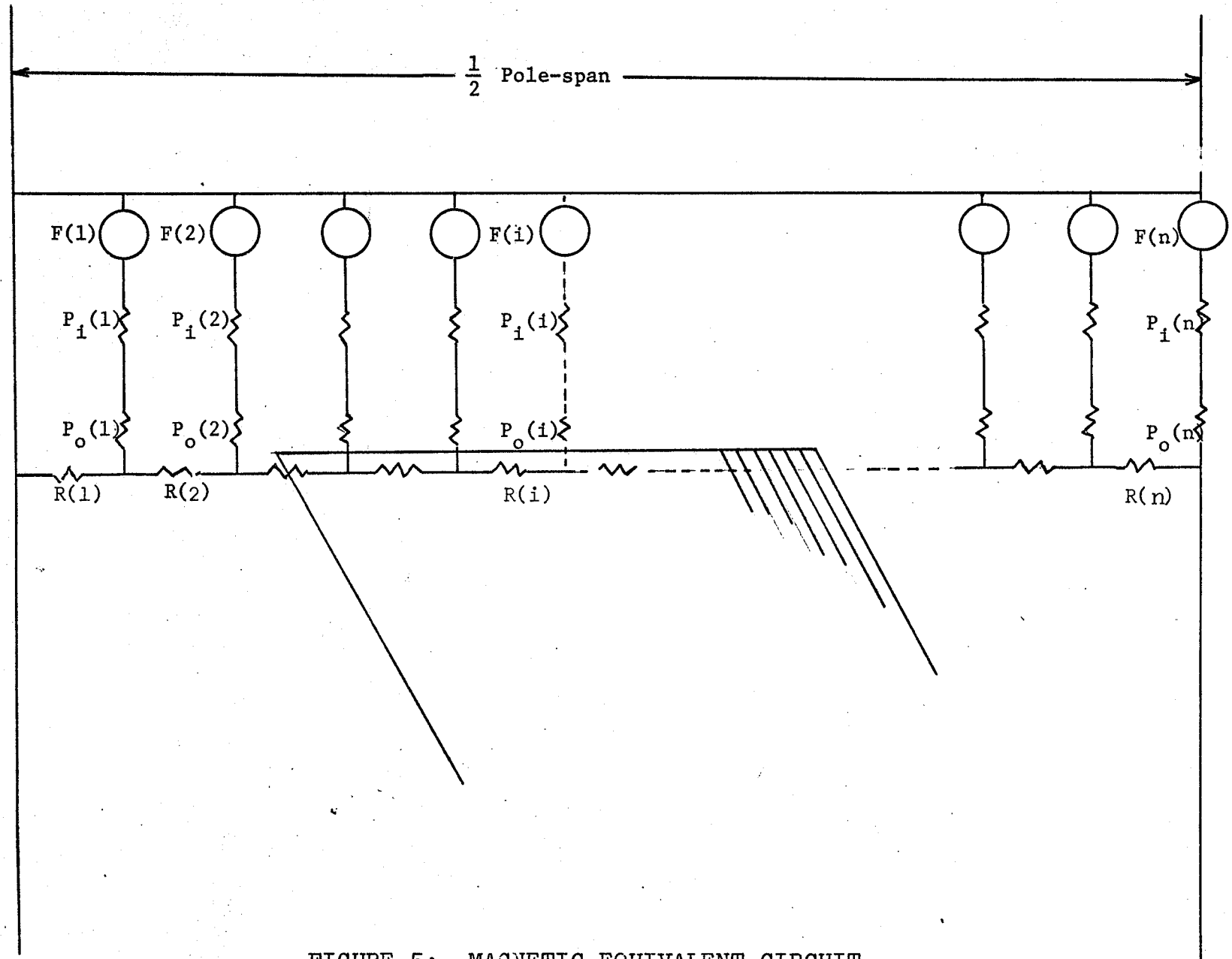

FIGURE 5: MAGNETIC EQUIVALENT CIRCUIT

Total relucatance was $R_T(i)$ where

$$R_T(i) = R_p(i) + R_n(i) \qquad ...(24)$$

As the magnetic equivalent lattice network was composed of similar section of such, the i-th row of the permeance matrix was as follows:

for i=j $$H(i,j) = \frac{1}{\frac{1}{P(i)} + \frac{R_n(i)\ R_p(i)}{R_T(i)}} \qquad ...(25)$$

for i=j+1<n $$H(i,j) = -\frac{Y(i)\ R_n(i-1)\ H(i-1,j)}{(1+Y(i))\ R_T(i-1)} \qquad ...(26)$$

for i>j+1<n $$H(i,j) = \frac{Y(i)\ H(i-1,j)}{(1+Y(i))\ Y(i-1)} \qquad ...(27)$$

for i=j+1=n $$H(i,j) = -\frac{R_n(i-1)\ H(i-1,j)}{R_T(i-1)} \qquad ...(28)$$

for i=n>j+1 $$H(i,j) = \frac{H(i-1,j)}{Y(i-1)} \qquad ...(29)$$

for i=j $$H(i,j) = H(j,i) \qquad ...(30)$$

given that $$Y(i) = P(i)\ R_p(i) \qquad ...(31)$$

From the matrix, it was possible to calculate the flux flowing on each leg of the lattice network and hence the flux density was calculated.

$$\phi(i) = \sum_{j=1}^{n} N(i,j)\ F(j) \qquad ...(32)$$

$$B(i) = \frac{\phi(i)}{A} \qquad ...(33)$$

Depending on whether the function of the flux

density distribution was even or odd, the function could be expressed in Fourier series form and the coefficients were, in discrete form:

$$C_N = \frac{4}{\pi} \sum_{m=1}^{n} m \varepsilon B(i) \cos N(m \varepsilon i) \qquad ...(34)$$

for odd function; ε is the angle subtended by each section.

The fundamental component of the flux density was found by making N=1. The coefficient C_1 was compared with the amplitude of the flux density of the cylindrical rotor. This ratio was also the ratio of the axis magnetising reactance to that of a cylindrical rotor.

2. CALCULATION OF NETWORK PARAMETER

Because of symmetry, only a section of the rotor needed to be considered. (As the chosen model of reluctance motor was a 4/8 pole stator, only one half of a quadrant of the rotor was considered.) The air gap periphery was divided into n equal sections. Each section subtended an angle ε given by

$$\varepsilon = \frac{\pi}{4n} \qquad ...(35)$$

The cross-sectional surface area was

$$A = \varepsilon r l \qquad ...(36)$$

3. MAGNETIC FLUX PATH

In an axially laminated anisotropic rotor, permeability in the direction of rolling is larger than in the

perpendicular directions. Hence the establishment of magnetic flux along the direction of rolling is easier.

There were two types of magnetic flux path across the air gap; flux either entering or leaving the pole-face and flux either entering or leaving the pole-side. The latter was the fringing effect. The flux path in this case was assumed to be a circular arc from the stator teeth surface to the side of the pole. The actual length of the path through the air gap in fringing effect involved quite a bit of geometry to calculate; however it contributed minutely to the calculation of flux density and so the accuracy of it was not critical.

CHAPTER III

SATURATION EFFECT

The study of saturation involved only the consideration of a region of the stator teeth. Saturation of the iron in this region occured before elsewhere in the stator core or the rotor because of the reduced volume due to slotting. The space factor was introduced for the purpose of relating the effect of the reduced volume. The slotting effect in the stator teeth was averaged for each section.

1. SPACE FACTOR

The region studied for saturation was the stator teeth region plus a region with a radial length, half the width of the teeth at the narrowest neck (see Figure 6). The extra region included was for fringing effect in the stator teeth and was a sort of 'rule of thumb' practice, without getting into sophisticated theory and calculation.

Considering the i-th section of the rotor, all the flux going through the air gap goes through the stator teeth region and the extended region.

$$\Phi(i) = B_o(i)\ A_o(i)$$

$$= B_i(i)\ A_i(i) \qquad \ldots(37)$$

where i denotes iron and o denotes air gap. B is the flux density and A is the cross-sectional area of the air gap at the stator teeth surface. The areas were not equal because

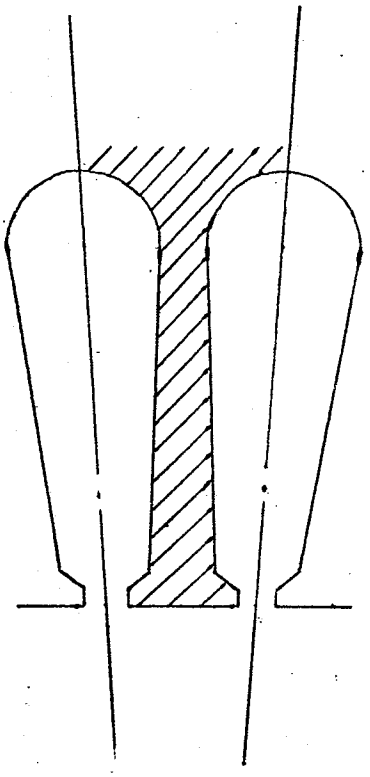

FIGURE 6: SATURATION REGION

of the slottings in stator iron.

$$B_i(i) = \frac{A_o}{A_i} B_o(i) \qquad ...(38)$$

$$S = \frac{A_o}{A_i} \qquad ...(39)$$

S was defined as the space factor.

Since the axial length of the rotor was common

$$S = \frac{l_o}{l_i} \qquad ...(40)$$

The calculation of the space factor was as follows. The total volume of the iron in the region was calculated and divided by the number of sections to get an average volume of iron in each section. This volume was then divided by the radial length of the region to get the circumferential length of iron in each section, i.e. l_o . From here, the space factor was calculated.

2. ADJUSTMENT AND CHECK

The adjustment and check were the two methods designed to get the saturated values of flux density using a computer. The magnet equivalent circuit method is based on the equation below:

$$\underline{\Phi} = P \, \underline{F} \qquad ...(41)$$

where P is the permeance matrix. Considering the i-th section, there was a magnetomotive force $F_o(i)$ acting across the air gap and $F_i(i)$ across the iron. The sum of these forces

was F(i); (assuming a zero rotor potential). The flux established in the air gap and the iron was the same. The calculation of this flux was based on equation (41). However, the permeance of the iron was a function of flux density in the iron and so considering saturation the non-linear variation of the iron permeance made it analytically difficult to calculate the flux density.

Figure 7 illustrates graphically, a method for the adjustment to get around the problem. The linear portion of the B-H curve was used to get the permeance of the unsaturated iron (the slope of line A in Figure 7). Calculation of the flux density was made. Starting with this value of flux density, the computer proceeded to locate the intersection of the curves B and C. The intersection point was the flux density of the saturated iron.

As a method to check the accuracy of the adjustment method, the result from the adjustment method was used to get the permeance of the saturated iron. (Given by slope of the line B'.) It was substituted as the permeance of iron in equation (41) and a calculation was made for the flux density. If the calculated value differed from the adjusted value by less than 0.1% the result was accepted.

The search for the intersection point converged and took an average of eight steps. There were points where the convergence would not take place. As the B-H curve was stored in the computer as a piece-wise linear curve, there were

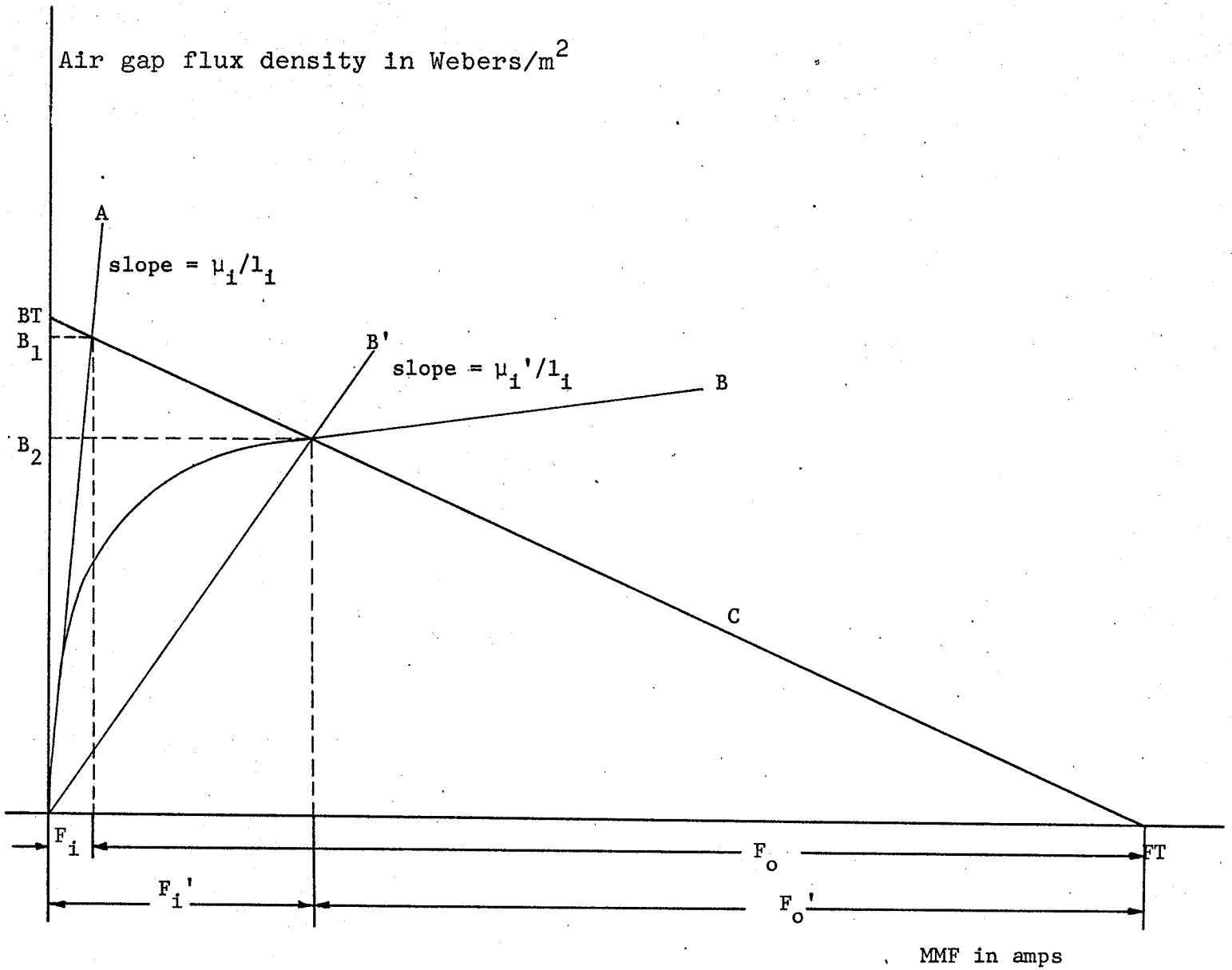

FIGURE 7: GRAPHIC REPRESENTATION OF SATURATION ADJUSTMENT METHOD

discontinuities and these were the points where no convergence existed, necessitating termination of the search. As discontinuities were undesirable, the number of piece-wise linear sections were limited. It should be pointed out that the B-H curve can be stored as a polynomial in the computer and so eliminated the need to break it down into piece-wise linear curves. This procedure was not seriously considered but should be in future studies.

When the rotor was in the quadrature-axis position, there was the rotor potential to be considered. Generally, the magnetomotive force across the air gap and the iron was the resultant magnetomotive force of the stator force and the rotor force. The adjustment method required that the resultant magnetomotive force be fixed. But as the rotor potential varied with the flux density, the resultant magnetomotive force could not be fixed. In this case, the resultant force was assumed fixed so that the adjustment process would be carried out. A value for the flux density was found. From this value, a new stator iron permeance was calculated and substituted into the check calculation. The two values were expectedly different and the cycle of adjusting and calculating was repeated using new values from each process for the next. In this was the result of the two values converged at a fast pace. In three cycles, the values were within 1% difference, for normal saturation conditions.

CHAPTER IV

CALCULATION OF AXIS REACTANCES

The program allowed for variation of several parameters. There was no attempt in this thesis to optimize the parameters. Synchronous performance of the machine for a given set of parameters was calculated. The following parameters are worth noting.

1. RADIAL AIR GAP LENGTH

This parameter was often referred to as the air gap. The measurement was done by taking the average of several readings of the outer diameter of the rotor and similarly for the inner diameter of the stator. The measuring instrument was within one-thousandth of an inch accurate or 0.03% error. (The diameter of the rotor was 100%.) Nevertheless, an error of 0.06% in the reading of the diameter would result in 3.3% error in the air gap length and consequently an error as high as 2% in the calculation of axis reactance could be expected.

The Carter coefficient was introduced to account for the fringing effect in the stator slots. There was no slotting in the rotor and any fringing effect in between the laminations was minimal because of the high stacking factor of the laminations.

The stacking factor along the axial length of the

stator was about 92% - 95%. Consequently, the magnetic axial length of the stator was shortened by 5%.

2. MEASUREMENT OF AXIS REACTANCES

The experimental model was an ordinary three-phase, 4/8 pole induction motor stator with a magnetically anisotropic rotor. Both a.c. and d.c. measurements were made for the axis reactances. The d.c. measurements were made based on a modified version of measuring self-inductance by J.C. Prescott and A.K. El-Kharashi[11]. A.c. measurements in the quadrature-axis position were impossible with the experimental set-up as this was the unstable region of the motor.

(a) Leakage Reactance:

This was an important parameter especially in the case of quadrature-axis reactance where the leakage reactance made up as much as 37% of the quadrature-axis reactance. A.c. and d.c. measurements were made on the motor with the rotor removed. When the rotor was removed for leakage reactance measurements, certain leakages were absent. These were the secondary slot leakages and zig-zag leakages. However, there was no slotting in the rotor and because the laminations in the rotor were thin, the amount of zig-zag leakage between the stator teeth and the rotor laminations would be very small. Single and three-phase a.c. measurements were taken for the 4 and 8 pole stator winding arrangement. The

single-phase measurements were lower than the three-phase measurements and the difference may be due to the absence of mutual flux leakage.

Several attempts were made to arrive at a method to calculate leakage reactance from machine dimensions[12]. However, the calculated results did not agree closely with the measured values. The specification from the manufacturer did not agree with the measured values either. Considering the importance of this parameter, the leakage reactance measured from the d.c. test was used as a compromise.

(b) Direct-Axis Reactances:

A.c. measurements were done assuming that the rotor aligned in the direct-axis position under light running condition.

$$Z_d = \frac{V_a}{I_{n.l.}} = (R_a^2 + X_d^2)^{1/2} = X_d \qquad ...(42)$$

where d is the direct-axis value, n.l. is no load and a is phase a. R_a, the resistance in phase a is usually small.

D.c. measurements were done with the rotor locked in the direct-axis position.

(c) Quadrature-Axis Reactances:

Using normal experimental set-up, a.c. measurement of quadrature-axis reactance is impossible because the quadrature-axis position is the unstable region of the machine. However, calculations of the axis reactance was made from the

terminal values of voltage, current and power when loads were applied to the motor running at synchronous speed[13]. The calculation gave a varied value of axis reactance for different loads. The variation diminished near pull-out region. That is, the region where the motor becomes overloaded and loses synchronism. D.c. measurements were done with the stationary rotor locked in the quadrature-axis position.

3. POWER FACTOR, STATOR CURRENT AND TORQUE

Calculations were made predicting the terminal characteristics of the motor from equations given in Chapter I, section 3. In the experiment, the power factor and stator current were measured at the machine terminals and the torque measured was the shaft torque. Hence, certain factors had to be looked into and accounted for.

(a) Windage Loss:

There was no simple method of calculating this loss although empirical methods were available. It was measured by a series of running light tests with different voltages. The power loss was plotted against the voltages. A line was drawn through these points until it intersected the zero voltage axis. The power reading at this axis was taken as the windage loss. This loss was subtracted from the calculated output torque to get the shaft torque.

(b) Iron Loss:

A simple way of calculating iron loss is given by P.L. Alger[14]. As the iron loss was proportional to the square of the voltage, the loss resistance was placed across the terminal. Experimentally, the iron loss was measured by subtracting the copper and windage losses from the total power loss in the running light test.

(c) X_d and X_q:

For a constant terminal voltage and assuming the winding resistance is small, the flux established in the air gap was the same for the rotor in the direct-axis position as in the quadrature-axis position. On that basis, the values of X_d and X_q were chosen for each voltage.

4. CALCULATION OF AXIS REACTANCES

Using the methods described in Chapter II and Chapter III, the flux density distributions in the air gap for the direct-axis and the quadrature-axis were calculated. A sketch of these distributions was plotted in Figure 8. The rotor positions and the fudamental components of the distributions were superimposed in the drawing. From the flux density distributions, the axis reactances were calculated for different excitations. These were plotted in Figures 9 and 10. The a.c. and d.c. measurements were also plotted against these curves for comparison.

The initial error in comparison was due to initial

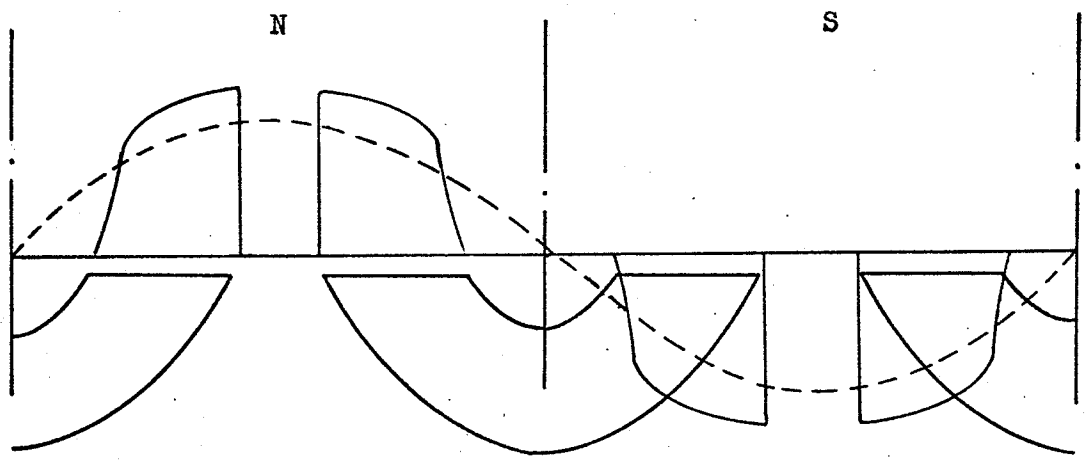

(a) Direct-Axis

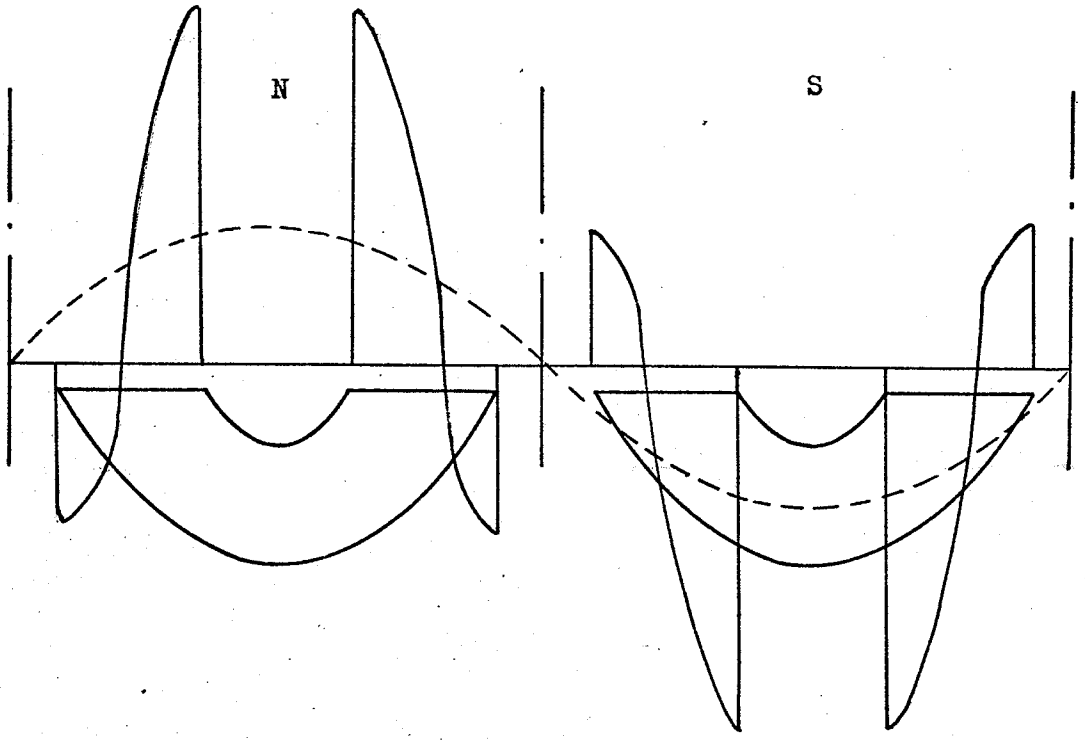

(b) Quadrature-Axis

FIGURE 8: FLUX DENSITY DISTRIBUTION

FIGURE 9: 4-POLE PLOT OF X_d AND X_q VS. I, STATOR CURRENT

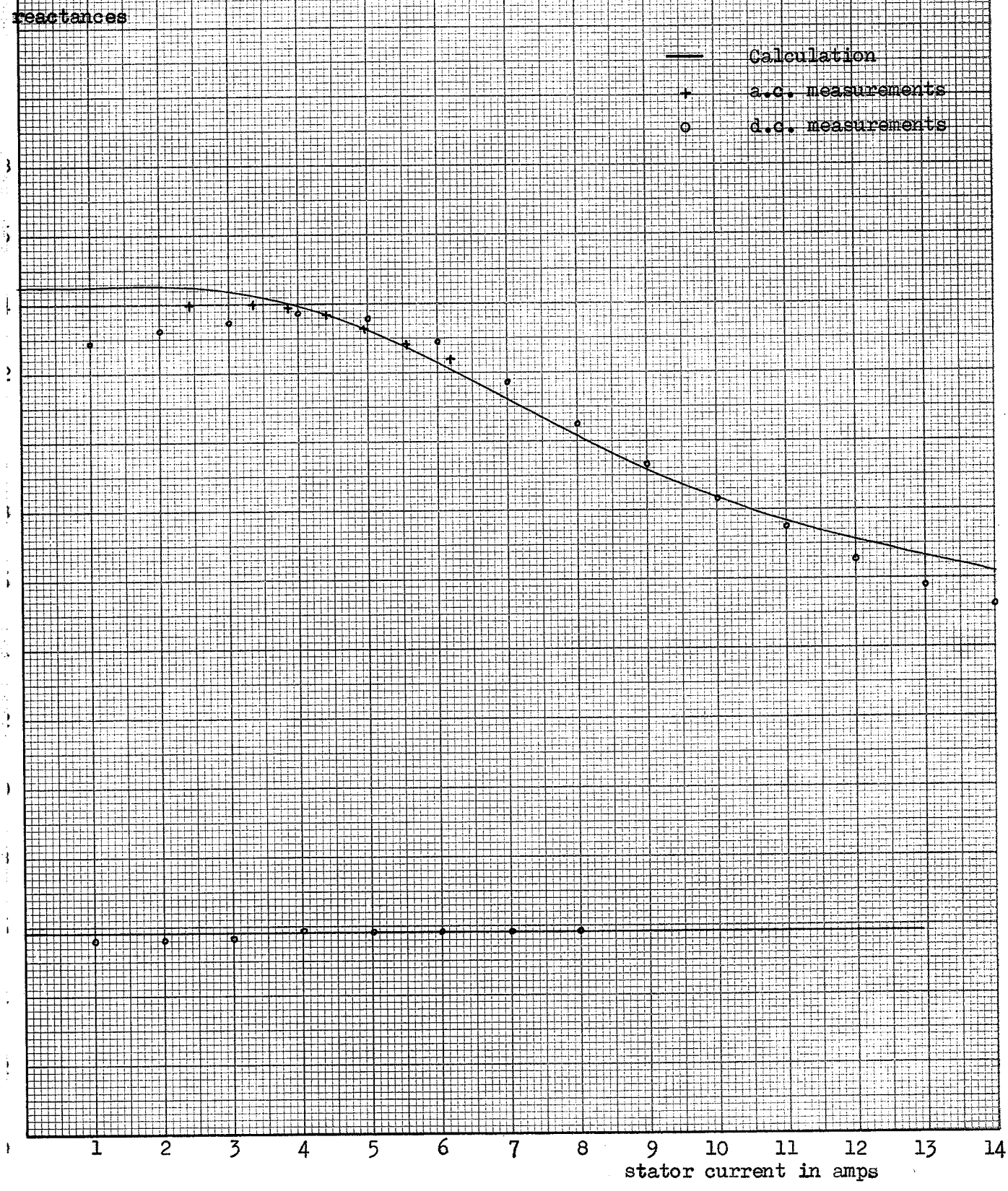

FIGURE 10: 8-POLE PLOT OF X_d AND X_q VS. I, STATOR CURRENT

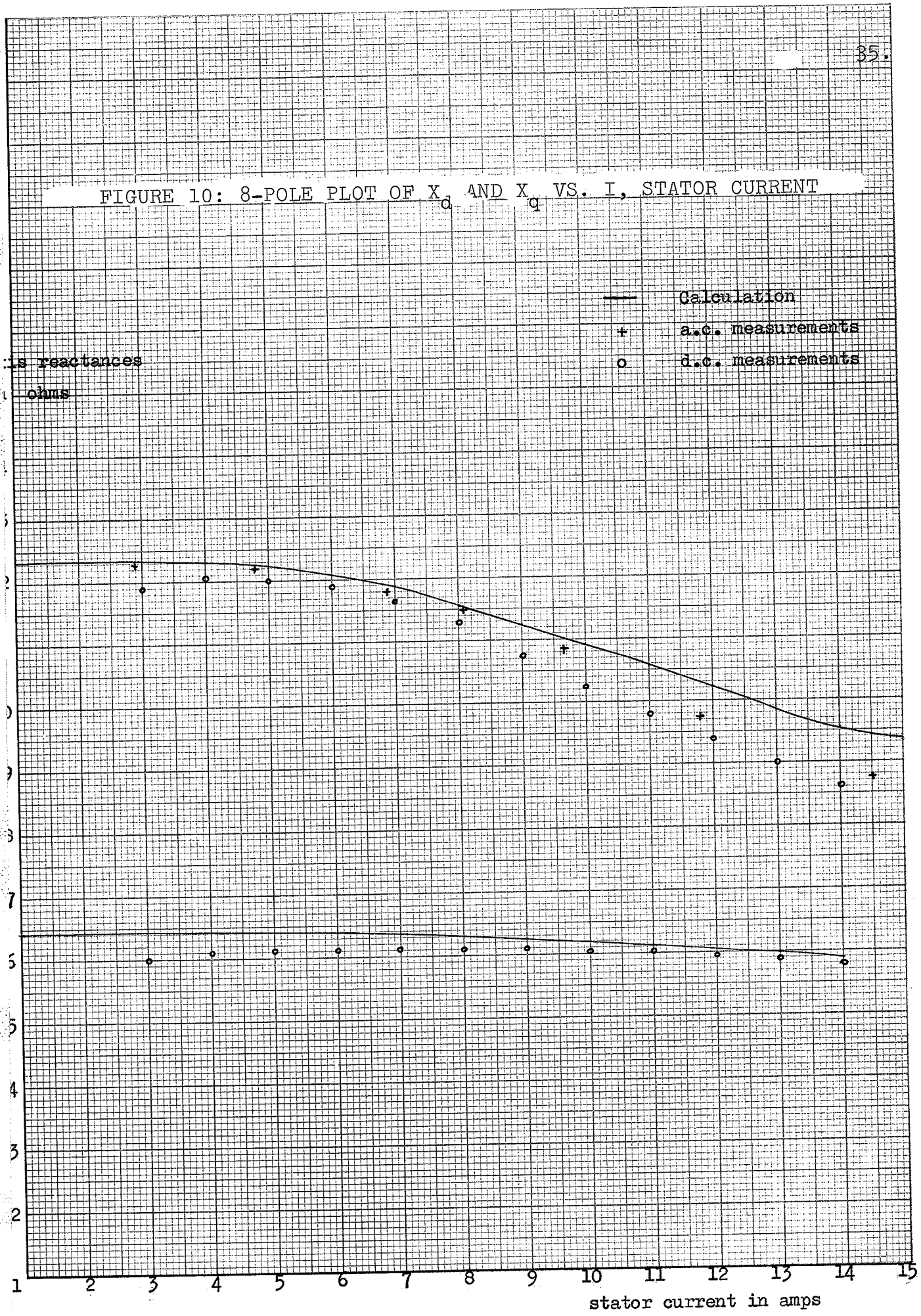

non-linearity of the magnetisation characteristic of the stator iron which was not modelled in the procedure. The saturation influence on the measured values of X_d at high excitation values was more than what was accounted for in the saturation region of the stator teeth. The agreement is very good over the operating range.

5. CALCULATION OF THE MACHINE SYNCHRONOUS PERFORMANCE

The calculation of the machine synchronous performance was plotted in Figures 11, 12 and 13. The measured value from a.c. tests were also plotted for comparison. The agreements were very good. The discrepancy was at worst, no more than 8%.

6. COMMENT

The excellent agreement between the measured and the calculated results for the axially laminated machine proved the validity of this mumerical method. Although the numerical method could be very accurate; the complexities involved such as machine boundary, anisotropic material and non-magnetic inter-laminal surfaces of rotor, would not justify the time and effort. The number of sections chosen was not very large. A study of the effect of the number of sections on the axis reactances showed that at the chosen number of sections, which was 45 sections, we were within 1% of the final value[15].

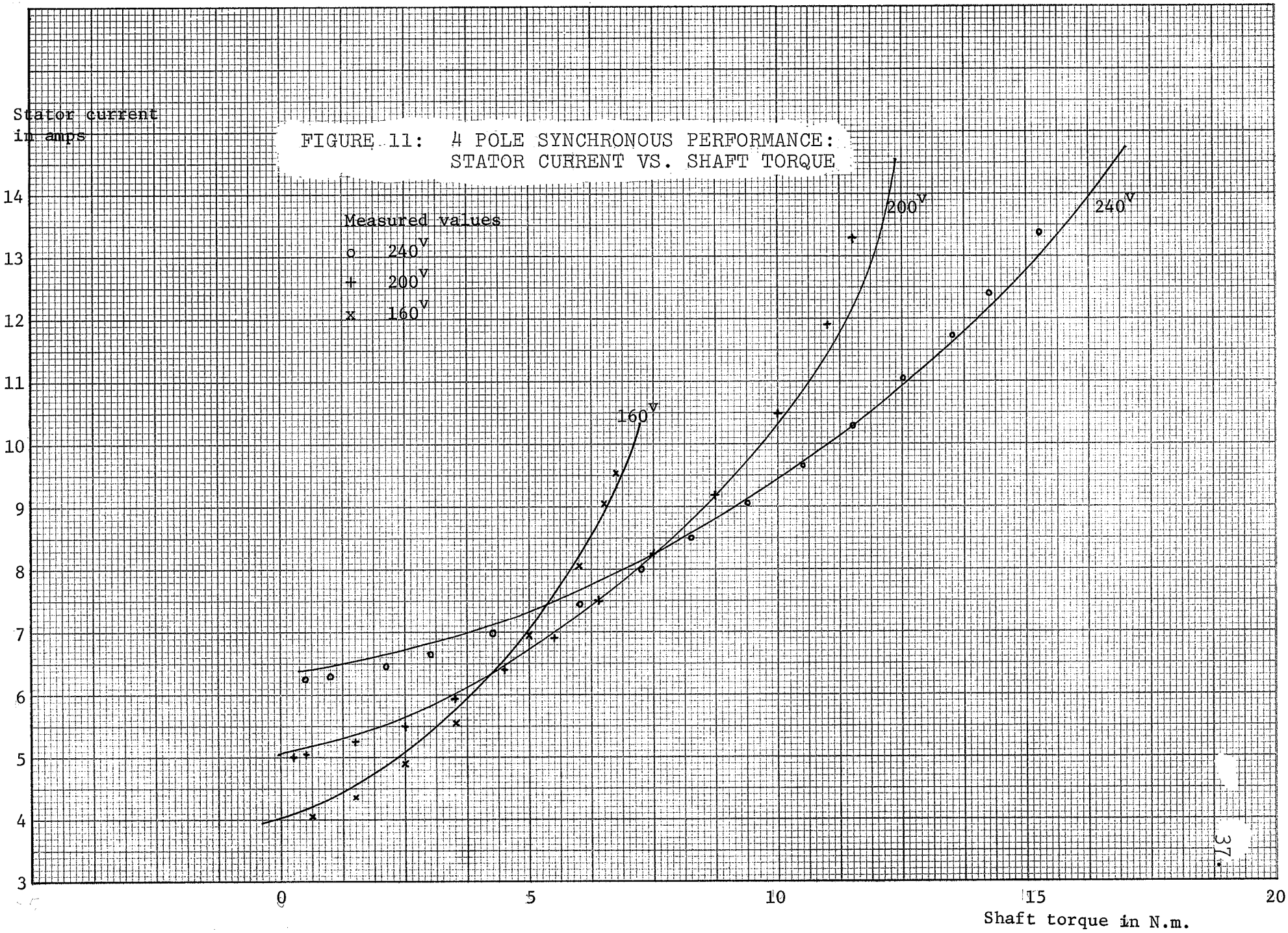
Stator current in amps
FIGURE 11: 4 POLE SYNCHRONOUS PERFORMANCE: STATOR CURRENT VS. SHAFT TORQUE
Measured values
o 240V
+ 200V
x 160V
160V
200V
240V
14
13
12
11
10
9
8
7
6
5
4
3
0
5
10
15
20
Shaft torque in N.m.

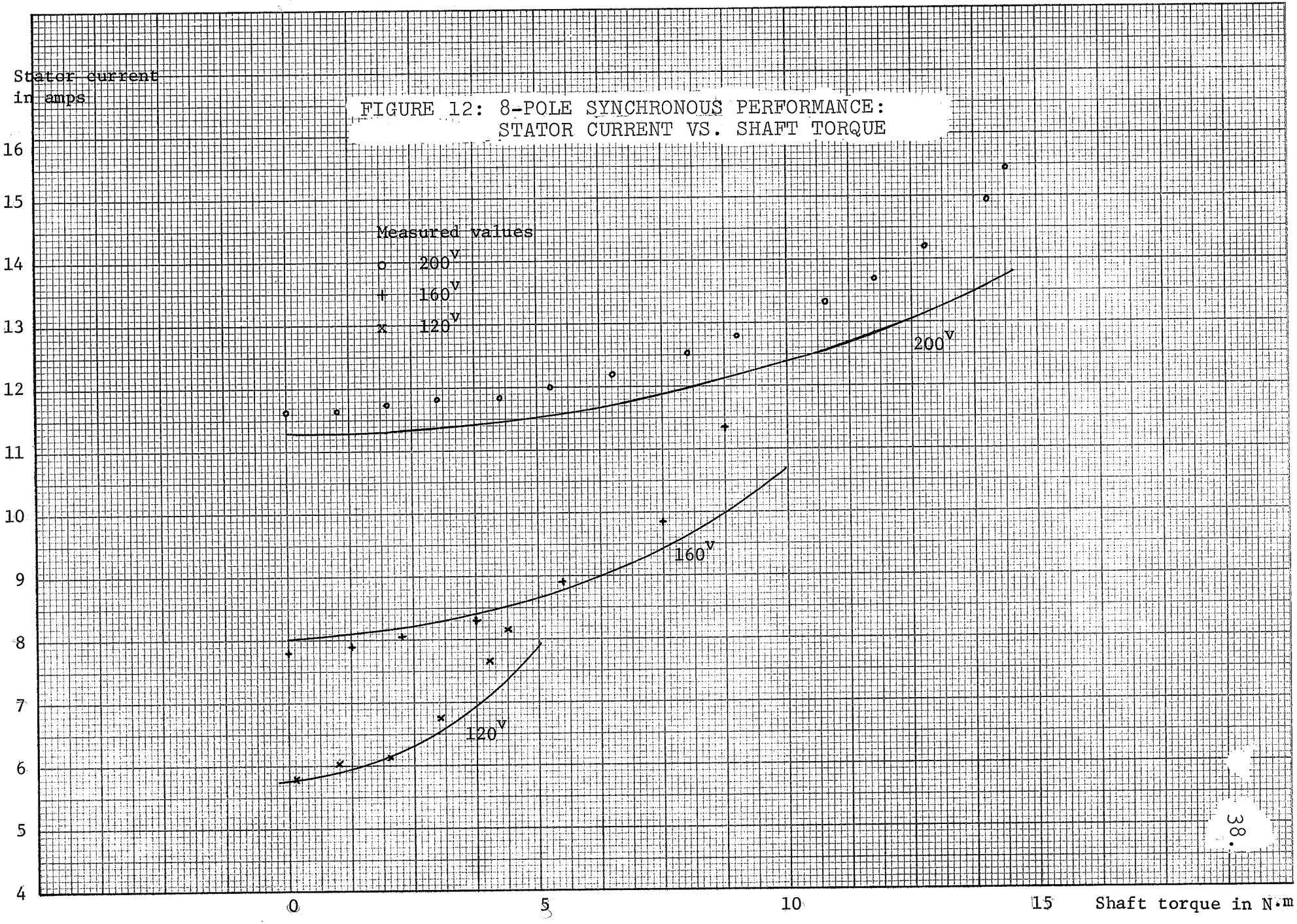
Stator current in amps
FIGURE 12: 8-POLE SYNCHRONOUS PERFORMANCE: STATOR CURRENT VS. SHAFT TORQUE
Measured values
o 200V
+ 160V
x 120V
200V
160V
120V
16
15
14
13
12
11
10
9
8
7
6
5
4
0
5
10
15
Shaft torque in N·m.

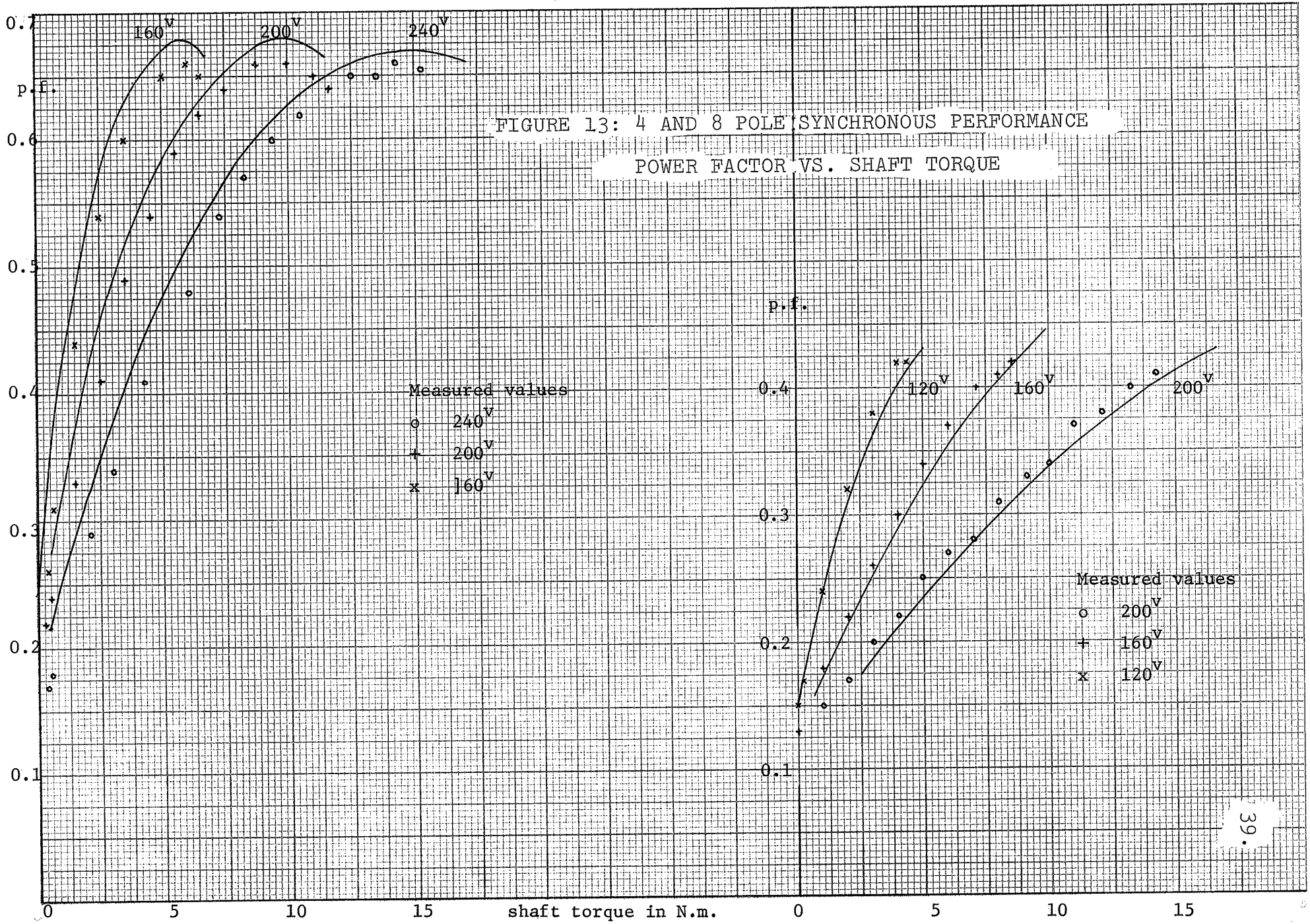
FIGURE 13: 4 AND 8 POLE SYNCHRONOUS PERFORMANCE
POWER FACTOR VS. SHAFT TORQUE
p.f.
0.7
0.6
0.5
0.4
0.3
0.2
0.1
160V
200V
240V
Measured values
o 240V
+ 200V
x 160V
0
5
10
15
shaft torque in N.m.
p.f.
0.4
0.3
0.2
0.1
120V
160V
200V
Measured values
o 200V
+ 160V
x 120V
0
5
10
15

This method is then simple and sufficiently general. It is not especially intended for anisotropic, axially laminated machines and is expected to hold for other reluctance machines with complex rotor shapes. It is a reliable method available to the designer of reluctance machines to reasonably predict the performances from design dimensions.

APPENDIX A

CALCULATIONS OF PERMEANCE AND RELUCTANCE OF ROTOR

Consider Figure 14, from the diagram

$$b(i) = r(\sin (45° - \theta(i) - \sin (45° - \rho))$$

$$a(i) = r(\cos (45° - \rho) - \cos (45° - \theta(i))$$

$$c(i) = a^2(i) + b^2(i)$$

$$\Gamma(i) = \tan^{-1} \left(\frac{b(i)}{a(i)}\right)$$

$$y(i) = c(i)\ \Gamma(i)$$

Consider the rotor in quadrature-axis position for $\theta > \sigma$; the permeance and reluctance in this section are

$$P(i) = \mu_o\ \varepsilon\ \frac{r}{g_1(i)}$$

$$g_1(i) = g + r\ (\theta(i) - \sigma)\ \frac{\pi}{2}$$

$$R(i) = \frac{\varepsilon}{\mu_o \cos\ (45° - \theta(i))}$$

for $\rho < \theta < \sigma$; the permeance and reluctance in this section are

$$P(i) = \mu_o\ \varepsilon\ \frac{r}{g}$$

$$R(i) = \left(\frac{s}{\mu} + \frac{1-s}{\mu_o}\right) \frac{\varepsilon \cos\ (45° - \theta(i))}{(\cos(45 - \theta(i)) - \cos 45) + \frac{\pi(\sin 45 - \sin(45-\theta(i))}{4}}$$

for $2° < \theta < \rho$; the permeance and reluctance in this section are

$$P(i) = \mu_o\ \varepsilon\ \frac{r}{g_2(i)}$$

$$g_2(i) = g + y(i)$$

$$R(i) = 0$$

for $\theta < 2°$; the permeance and reluctance in this section are

$$P(i) = \mu_o \varepsilon \frac{r}{g_3(i)}$$

$$g_2(i) = g + \frac{3"}{8} \times 0.0254$$

$$R(i) = 0$$

where s is the stacking factor. If the rotor is at direct-axis position, the permeance is the same as in the case of the quadrature-axis except for the reluctance which is zero throughout.

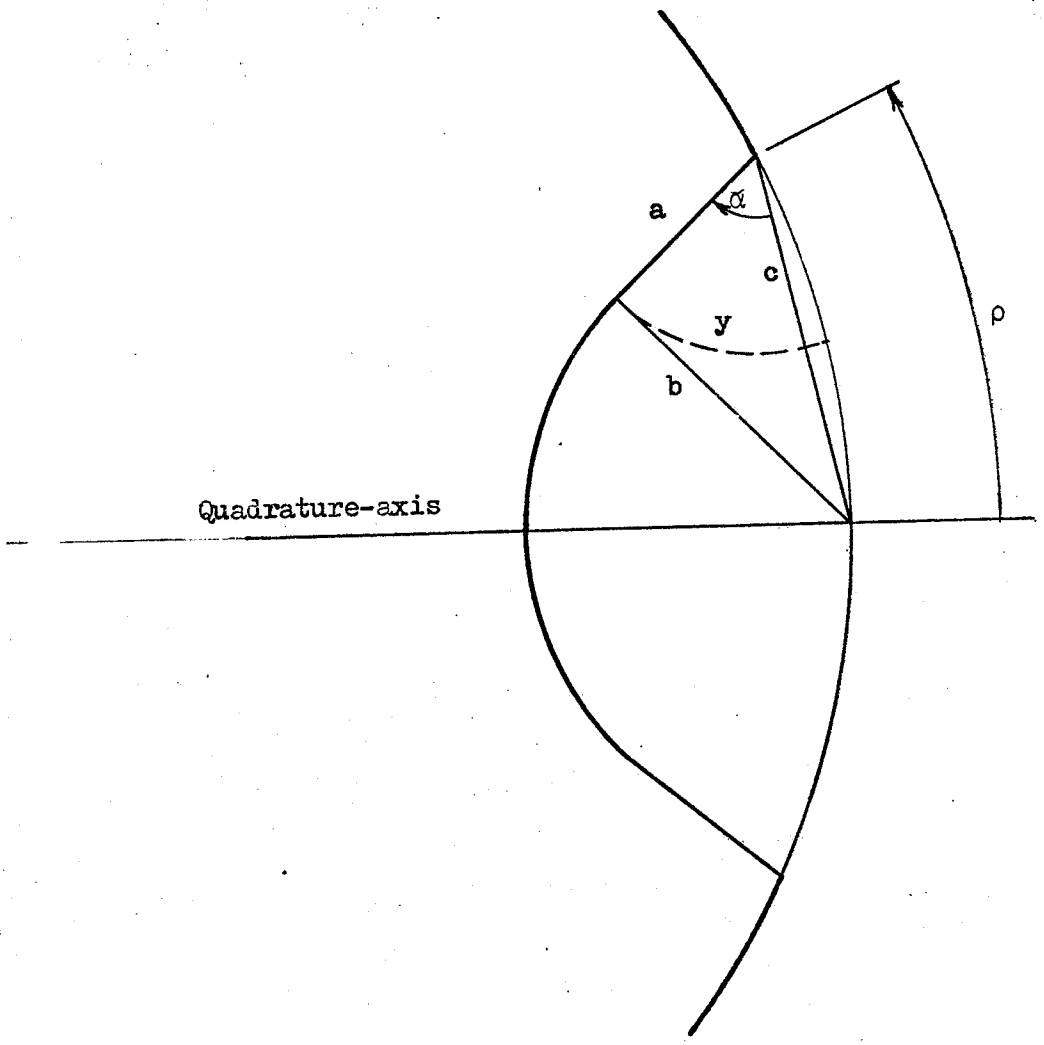

FIGURE 14: CALCULATION OF MAGNETIC PATH LENGTH

APPENDIX B

THE EXPERIMENTAL MACHINE

The following data were taken from the specifications of the three-phase, 4/8 pole experimental reluctance motor with axially laminated rotor:

Number of slots	48 semi-closed, no skew
Number of coils	48
Number of conductors per slot	46
Number of turns per coil	23
Coil pitch	1 - 7
Radius of rotor	76.2 mm
Core length	101.6 mm
Air gap length	0.762 mm
Stator teeth length	28.1 mm
Stacking factor	95%
Permeability of iron:	
in direction of easy magnetisation	0.005 newton/amp^2
in perpendicular directions	0.0001 newton/amp^2
Inner limit of laminations	20° el.
Outer limit of laminations	72° el.
Lamination thickness	0.33 mm
Number of sections of lattice network	45
Winding arrangement	parallel-star

Single phase resistance of winding	0.676 ohm
Single phase leakage reactance	2.04 ohms (4 pole)
	1.885 ohms (8 pole)

APPENDIX C

COMPUTER PROGRAM

```
// JOB   X    X 10.010 HRS
// FOR AXIS
*IOCS(DISK,TYPEWRITER)
*LIST SOURCE PROGRAM
      COMMON H(45,45),F(45),FLUX(45),B(45),P(45),R(45),RPL(45),RNL(45),
     1RLT(45),Y(45),UO,PI,GE(45),UR1(45),N
C     ****************************************************************
C     MAIN PROGRAM          THIS PROGRAM CALLS FUNCTIONS CKD AND CKQ
C     WHICH IN TURN CALL FUNCTION CKR AND SUBROUTINE MATRIX.  THE
C     MACHINE DIMENSIONS AND CONSTANTS ARE READ INTO THE MAIN PROGRAM.
C     CARTER COEFFICIENT IS CALCULATED AND IS USED TO DETERMINE THE
C     EFFECTIVE AIR GAP LENGTH IN THE MOTOR.  THE MAGNETISING REACTANCE
C     OF THE CYLINDRICAL ROTOR AND THE MAGNETOMOTIVE FORCE
C     OF THE CYLINDRICAL ROTOR AND THE R.M.S. VALUE OF THE MMF AT THE
C     AIR GAP ARE CALCULATED.  THE MAIN PROGRAM THEN CALLS THE FUNCTIONS
C     WHICH CALCULATE THE DIRECT-AXIS AND QUADRATURE-AXIS MAGNETISING
C     REACTANCES.
C     GA       AIR GAP LENGTH
C     UO       PERMEABILITY CONSTANT OF AIR
C     G        EFFECTIVE AIR GAP LENGTH
C     CART     CARTER COEFFICIENT
C     CLG      STATOR CORE LENGTH
C     FT       RMS VALUE OF MMF
C     A        CROSS-SEC)IONAL AREA OF A   SECTION
C     C        EXCITING CURRENT
C     ****************************************************************
C
C     CONSTANTS AND MACHINE DIMENSIONS
      READ (5,6)D,FT,U,S,PP,PT,PH
    6 FORMAT (2F10.6   /2F10.6/3F10.6)
      PI=3.14159
      UO=4.*PI*1.E-7
      SLOT=2.54*1.E-3
      TEETH=(2.*D*PI)/48.-SLOT
      READ (5,5) GA,CK
    5 FORMAT (2F10.4)
   29 GA=GA*0.0254
      CART= (SLOT+TEETH)/(SLOT+TEETH-CK  *SLOT)
   21 G=GA*CART
      TEATA=2.*PI/180.
      SIG=38./180.*PI
      RHO=9.8/180.*PI
      W=120.*PI
      CLG=0.0254*4.*0.95
      WDF=0.707
      WDP=0.959
      TRN=92.
      RT=TRN*TRN*WDF*WDF*WDP*WDP
      XM   =(6.*RT*W*CLG*D*UO)/(G   *PI)
      N=45
      C=6.17
      FT=FT*C
      CC = UO*FT/G
      DEL=PI/(4.*N)
      RR = DEL/UO
      A = D*DEL
      PR = UO*DEL
      PO = PR*D/G
      T=PI/4.
      DKD=CKD(  T,DEL,PR,PO,SIG,RHO,FT,D,G,A,CC,PP,TEATA,PT,PH,RR,GA,C,X
     1M)
      ET=FT/C
   22 CALL EXIT
      END
```

0933534

```
/
 / JOB   X    X 11.671 HRS
// FOR AXIS
*IOCS(DISK,TYPEWRITER)
*LIST SOURCE PROGRAM
C     ******************************************************************
C     FUNCTION CKD IS CALLED BY MAIN PROGRAM.  IT IN TURN CALLS THE
C     PERMEANCES AND RELUCTANCES FOR EACH SECTION OF THE MAGNETIC
C     LATTICE NETWORK.  IT THEN CALLED THE SUBROUTINE MATRIX TO SET UP
C     THE MATRIX AND THEN RETURNS AND CALCULATES THE FLUX DENSITY OF THE
C     AIR GAP IN EACH SECTION.  IT THEN CALLED THE FUNCTION CKR TO MAKE
C     THE ADJUSTMENT FOR SATURATION.
C     SRR      RADIUS OF THE CIRCULAR GAP IN THE ROTOR
C     EM       SPACE FACTOR
C     FELG     LENGTH OF IRON IN THE SATURATED REGION
C     UR1      RELATIVE PERMEABILITY OF IRON
C     B        FLUX DENSITY
C
C
C
C     ******************************************************************
      FUNCTION CKD(  T,DEL,PR,PO,SIG,RHO,FT,D,G,A,CC,PP,TEATA,PT,PH,RR,G
     1A,C,XM)
      COMMON H(45,45),F(45),FLUX(45),B(45),P(45),R(45),RPL(45),RNL(45),
     1RLT(45),Y(45),UO,PI,GE(45),UR1(45),N
      SRR=3./8.*0.0254
      EM=2.
      FELG=1.173*0.0254*EM
      TRIAK=1.
      DO 14 I=1,N
   14 UR1(I)=.00725/UO
  178 TRIAK=TRIAK+1.
C     SETS UP PERMEANCES AND RELUCTANCES FOR EACH SECTION.
      DO 10 I=1,N
      T = T-DEL
      TT=T+DEL/2.
    3 IF(T-SIG) 1,1,2
    2 RLG=FELG/(GA+PI*D*(T-SIG)/2.)
      GE(I)=GA+PI*D*(T-SIG)/2.
      FEFAC=RLG/UR1(I)
      P(I)=PR*D/(GE(I)*(1.+FEFAC))
      R(I)=1.E-30
      GO TO 10
    1 IF(T-RHO) 4,5,5
    5 RLG=FELG/G
      FEFAC=RLG/UR1(I)
      GE(I)=G
      P(I)=PO/(1+FEFAC)
      R(I)=1.E-30
      GO TO 10
    4 IF (T-TEATA) 11,11,22
   22 PRP=SIN(PI/4.-T)-SIN(PI/4.-RHO)
      PPR=COS(PI/4.-RHO)-COS(PI/4.-T)
      ALPHA=ATAN(PRP/PPR)
      PB=D*SQRT(PRP*PRP+PPR*PPR)
      GE(I)=GA+ALPHA*PB
      RLG=FELG/GE(I)
      FEFAC=RLG/UR1(I)
      P(I)=PR*D/(GE(I)*(1.+FEFAC))
      R(I)=1.E-30
      GO TO 10
   11 GE(I)=GA+SRR
      RLG=FELG/GE(I)
      FEFAC=RLG/UR1(I)
      P(I)=PR*D/(GE(I)*(1.+FEFAC))
      R(I)=1.E-30
```

```
   10 F(I)=FT*SIN(PT*TT)
C     CALCULATES  THE AIR GAP FLUX DENSITY
      CALL MATRIX
      DO 44 L=1,N
      FLUX(L) =0.0
      DO 55 M=1,N
   55 FLUX(L) = FLUX(L)+H(L,M)*F(M)
      B(L)=FLUX(L)/A
   44 CONTINUE
      CB=0.
      PS=1.
C     ZEROES THE FRINGING FLUX AT THE MAGNETIC POTENTIAL AXIS
      K=N
      JJ=10*N/45
      JK=JJ+1
      BB=JJ
      BO=B(K)/BB
      DO 855 J=1,JJ
      B(K)=B(K)-BO*(JK -J)
      K=K-J
  855 CONTINUE
      DO 66 LL=1,N
   66 CB=CB+4.*PH*DEL*B(LL)*COS(PS*(PP*LL-1.)*DEL)/PI
      CKC=CB/CC
      DXD=CKC*XM
      WRITE(6,13) PS,CB,CKC,DXD
      T=PI/4.
      CKD=CKR(  T,DEL,PR,PO,SIG,RHO,FT,D,G,A,CC,PP,TEATA,PT,PH,RR,GA,EM)
      K=N
      JJ=10*N/45
      JK=JJ+1
      BB=JJ
      BO=B(K)/BB
      DO 955 J=1,JJ
      B(K)=B(K)-BO*(JK -J)
      K=K-J
  955 CONTINUE
C     USES FOURIER SERIES TO GET THE FUNDAMENTAL COMPONENT OF THE FLUX
C     DENSITY
      CB=0.
      DO65 LL=1,N
   65 CB=CB+4.*PH*DEL*B(LL)*COS(PS*(PP*LL-1.)*DEL)/PI
C     CALCULATE AXIS MAGNETIC REACTANCE
      CKC=CB/CC
      DXD=CKC*XM
      WRITE(6,13) PS,CB,CKC,DXD
   13 FORMAT(4F10.4)
      WRITE (6,16)N,EM ,C
   16 FORMAT (I4,2F10.4//)
      RETURN
      END
```

```
// JOB   X    X 13.046 HRS
// FOR AXIS
*IOCS(DISK,TYPEWRITER)
*LIST SOURCE PROGRAM
C     ******************************************************************
C     FUNCTION CKQ IS CALLED BY MAIN PROGRAM.  IT IN TURN CALLS THE
C     PERMEANCES AND RELUCTANCES FOR EACH SECTION OF THE MAGNETIC
C     LATTICE NETWORK.  IT THEN CALLED THE SUBROUTINE MATRIX TO SET UP
C     THE MATRIX AND THEN RETURNS AND CALCULATES THE FLUX DENSITY OF THE
C     AIR GAP IN EACH SECTION.  IT THEN CALLED THE FUNCTION CKR TO MAKE
C     THE ADJUSTMENT FOR SATURATION.
C     FUNCTION CKQ IS SIMILAR TO FUNCTION CKD WITH THE EXCEPTION THAT
C     THE ITERATIVE PROCESS IS REPEATED SEVERAL TIME.
C     SRR      RADIUS OF THE CIRCULAR GAP IN THE ROTOR
C     EM       SPACE FACTOR
C     FELG     LENGTH OF IRON IN THE SATURATED REGION
C     UR1      RELATIVE PERMEABILITY OF IRON
C     B        FLUX DENSITY
C
C     ******************************************************************
C
C
      FUNCTION CKQ(  T,DEL,PR,PO,SIG,RHO,FT,D,G,A,CC,U,S,RR,PP,TEATA,PT,
     1PH,GA,C,XM)
      COMMON H(45,45),F(45),FLUX(45),B(45),P(45),R(45),RPL(45),RNL(45),
     1RLT(45),Y(45),UO,PI,GE(45),UR1(45),N
      RLR=(UO*S+U*(1.-S))/(U*UO)
      EM=2.
      TRIAK=0.
      DO 14 I=1,N
   14 UR1(I)=.00725/UO
      SRR=3./8.*0.0254
  178 TRIAK=TRIAK+1.
      FELG=1.173*0.0254*EM
C     SETS UP PERMEANCES AND RELUCTANCES FOR EACH SECTION.
      DO 10 I=1,N
      T = T-DEL
      TT=T+DEL/2.
    3 IF(T-SIG) 1,1,2
    2 RLG=FELG/(GA+PI*D*(T-SIG)/2.)
       GE(I)=GA+PI*D*(T-SIG)/2.
      FEFAC=RLG/UR1(I)
       P(I)=PR*D/(GE(I)*(1.+FEFAC))
      R(I)=RR/COS(PI/4.-T)
      GO TO 10
    1 IF(T-RHO) 4,5,5
    5 RLG=FELG/G
      FEFAC=RLG/UR1(I)
      GE(I)=G
      P(I)=PO/(1+FEFAC)
      RRL=COS(PI/4.-T)-0.707+(0.707-SIN(PI/4.-T))*PI/4.
      RL=RLR*DEL*COS(PI/4.-T)/RRL
      R(I) = RL
      GO TO 10
    4 IF (T-TEATA) 11,11,22
   22 PRP=SIN(PI/4.-T)-SIN(PI/4.-RHO)
      PPR=COS(PI/4.-RHO)-COS(PI/4.-T)
      ALPHA=ATAN(PRP/PPR)
      PB=D*SQRT(PRP*PRP+PPR*PPR)
      GE(I)=GA+ALPHA*PB
      RLG=FELG/GE(I)
      FEFAC=RLG/UR1(I)
      P(I)=PR*D/(GE(I)*(1.+FEFAC))
      R(I)=1.E-30
      GO TO 10
   11 GE(I)=GA+SRR
      RLG=FELG/GE(I)
      FEFAC=RLG/UR1(I)
      P(I)=PR*D/(GE(I)*(1.+FEFAC))
      R(I)=1.E-30
   10 F(I)=FT*COS(PT*TT)
C     CALCULATES  THE AIR GAP FLUX DENSITY
      CALL MATRIX
      DO 44 L=1,N
      FLUX(L) =0.0
      DO 55 M=1,N
   55 FLUX(L) = FLUX(L)+H(L,M)*F(M)
      B(L)=FLUX(L)/A
   44 CONTINUE
      CA=0.
      PS=1.
      DO 66 LL=1,N
   66 CA=CA+4.*PH*DEL*B(LL)*SIN(PS*(PP*LL-1.)*DEL)/PI
      CKC=CA/CC
      DXQ=CKC*XM
      WRITE(6,13) PS,CA,CKC,DXQ
   13 FORMAT (4F10.4)
  444 T=PI/4.
      CKQ=CKR(  T,DEL,PR,PO,SIG,RHO,FT,D,G,A,CC,PP,TEATA,PT,PH,RR,GA,EM)
      CA=0.
      PS=1.
C     USES FOURIER SERIES TO GET THE FUNDAMENTAL COMPONENT OF THE FLUX
C     DENSITY
      DO 65 LL=1,N
   65 CA=CA+4.*PH*DEL*B(LL)*SIN(PS*(PP*LL-1.)*DEL)/PI
      CKC=CA/CC
      DXQ=CKC*XM
      WRITE(6,13) PS,CA,CKC,DXQ
      T=PI/4.
      IF(TRIAK.LT.3.) GO TO 178
      WRITE (6,8)N,EM,C
    8 FORMAT(I4,2F10.4//)
      RETURN
      END
```

```
// JOB   X    X 11.422 HRS                                                5]
// FOR AXIS
*IOCS(DISK,TYPEWRITER)
*LIST SOURCE PROGRAM
C     ********************************************************************
C     FUNCTION CKR STORES THE B-H CHARACTERISTIC OF IRON AND WITH THE
C     RESULT FROM FCN CKD OR CKQ, IT LOCATES THE INTERSECTION OF TWO
C     CURVES
C     BFI=EQUIVALENT FLUX DENSITY OF AIR IN IRON
C     HFE=FIELD INTENSITY IN IRON
C     FO=EQUIVALENT FIELD DENSITY OF AIR
C     EM=SPACE FACTOR
C     FF=TOTAL FIELD INTENSITY
C     GE=AIR GAP LENGTH
C     FELG=LENGTH OF IRON
C     ********************************************************************
      FUNCTION CKR(  T,DEL,PR,PO,SIG,RHO,FT,D,G,A,CC,PP,TEATA,PT,PH,RR,G
     1A,EM)
      COMMON H(45,45),F(45),FLUX(45),B(45),P(45),R(45),RPL(45),RNL(45),
     1RLT(45),Y(45),UO,PI,GE(45),UR1(45),N
C     SATURATION ADJUSTMENT TO IRON
C     UR1=0.00725
C     UR2=0.002625
C     UR3=0.001425
C     UR4=0.00123
C     UR5=0.000654
C     UR6=0.000516
C     UR7=0.000352
C     UR8=0.000216
C     UR9=0.0001475
C     UR10=.000109
C     UR11=.0000948
C     UR12=.0000606
C     UR13=0.0000407
C     B-H CURVE OF IRON
      B2=.4134
      B3=.59
      B4=.631
      B5=.8039
      B6=.866
      B7=.9925
      B8=1.0985
      B9=1.1912
      B10=1.267
      B11=1.2995
      B12=1.4008
      B13=1.528
      FELG=0.0254*1.173
      FA=1.E-30
      DO 61 I=1,N
      FB=B(I)
      B(I)=ABS(B(I))
      BFI=EM*B(I)
      IF(BFI-.6484)21,21,133
      IMY=2
  133 HFE=BFI/UR1(I)*UO
      ITER=0.
      HON=0.5
      BG=B(I)
C     B-H LINE OF AIR
      FF=ABS(FLUX(I)/P(I))
      GG=GE(I)
      BT=UO*FF/GG
```

```
      BE=100.
C     SEEKS THE INTERSECTION OF TWO CURVES                          0933601
   15 IF(HFE-147.3)50,50,51                                         52
   50 BFI =2.625*HFE*1.E-3+B2
      GO TO 41
   51 IF(HFE-210.8)52,52,53
   52 BFI =1.425*HFE*1.E-3+B3
      GO TO 41
   53 IF(HFE-299.8)54,54,56
   54 BFI =1.23*HFE*1.E-3+B4
      GO TO 41
   56 IF(HFE-452.8)57,57,58
   57 BFI =.654*HFE*1.E-3+B5
      GO TO 41
   58 IF(HFE-646.8)59,59,70
   59 BFI =.516*HFE*1.E-3+B6
      GO TO 41
   70 IF(HFE-930.8)71,71,72
   71 BFI =.352*HFE*1.E-3+B7
      GO TO 41
   72 IF(HFE-1416.7)73,73,74
   73 BFI =.216*HFE*1.E-3+B8
      GO TO 41
   74 IF(HFE-1958.)75,75,76
   75 BFI =.1475*HFE*1.E-3+B9
      GO TO 41
   76 IF(HFE-2325.)77,77,78
   77 BFI =.109*HFE*1.E-3+B10
      GO TO 41
   78 IF(HFE-2958.)79,79,80
   79 BFI =.0948*HFE*1.E-3+B11
      GO TO 41
   80 IF(HFE-3750.)81,81,82
   81 BFI =.0606*HFE*1.E-3+B12
      GO TO 41
   82 BFI =.0407*HFE*1.E-3+B13
   41 B(I)=BFI/EM
      IF (ITER-100)42,4 ,4
   42 ITER=ITER+1
   62 BI=B(I)
      BF=ABS(BG-BI)
      IF (BF-0.0001)4,4,3
    3 IF (HON.GT.1.0) GO TO 17
      IF (BF.GT.BE) GO TO 17
      BG=(BG+BI)/2.
      BE=BF
      FO=BG*GG/UO
      FI=FF-FO
   18 HFG=HFE
      HFE=FI/FELG
      WRITE(6,134)HFE,IMY,I,HON
  134 FORMAT (E16.8,2I4,F10.4)
      GO TO 15
   17 HON=1.5
      IF (BG.GT.BI) GO TO 90
      HINC=ABS((HFE-HFG)/2.)
      HFF=HFE
   27 HFE=HFE-HINC*1.5
      GO TO 96
   90 HINC=ABS((HFF-HFE)/2.)
      HFG=HFE
   91 HFE=HFE+HINC
   96 FI=HFE*FELG
      FO=FF-FI
      BG=FO*UO/GG
      WRITE(6,134)HFE,IMY,I,HON
      GO TO 15
    4 UR1(I)=BFI/(HFE*UO)                                           0933602
   21 IF (FB-FA) 14,14,61
   14 B(I)=-B(I)
   61 CONTINUE
      RETURN
      END
```

```
// JOB   X     X 12.819 HRS
// FOR AXIS
*IOCS(DISK,TYPEWRITER)
*LIST SOURCE PROGRAM
C     ************
  12.821  CARD00  NOT READY   BP-ROR  FF16  7A45  7A56  1000  0801  0003  OR
*******************************************************
C     SUBROUTINE MATRIX IS CALLED BY FUNCTION CKD AND CKQ
C     ********************************************************************
      DO 3 I=1,N
      II=N+1-I
      IF(I.GT.1) GO TO 5
      RNL(I)=R(I)
      RPL(II)=1.E30
      GO TO 3
    5 RNL(I)=R(I)+1./(P(I-1)+1./RNL(I-1))
      RPL(II)=R(II+1)+1./(P(II+1)+1./RPL(II+1))
    3 CONTINUE
      DO 6 I=1,N
      Y(I)=RPL(I)*P(I)
    6 RLT(I)=RPL(I)+RNL(I)
      DO 7 J=1,N
      DO 7 K=1,N
      KK=K-1
      IF(K-J) 11,22,33
   22 H(K,J)=1./(1./P(K)+RPL(K)*RNL(K)/RLT(K)    )
      GO TO 7
   33 IF(KK-J) 31,31,32
   31 IF (K-N) 34,35,35
   34 H(K,J)=- Y(K)*RNL(KK)*H(KK,J)/((1.+Y(K))*RLT(KK))
      GO TO 7
   35 H(K,J)=-RNL(KK)*H(KK,J)/RLT(KK)
      GO TO 7
   32 IF(K-N) 37,38,38
   37 H(K,J)=Y(K)*H(KK,J)/((1.+Y(K))*Y(KK))
      GO TO 7
   38 H(K,J)= H(KK,J)/ Y(KK)
      GO TO 7
   11 H(K,J)=H(J,K)
    7 CONTINUE
      RETURN
      END
```

REFERENCES

1. Lawrenson, P.J. "The importance of reluctance motors", Design Eng., May 1969, pp 89-92.

2. Kostko, J.K. "Polyphase reaction synchronous machine", Jour. AIEE, Nov 1923, pp 1162.

3. Risch, N.O. "Segmental rotor core lamination for use in synchronous induction motors", U.S. Patent 2,769,108, 1956.

4. Cruickshank, A.J.O., Menzies, R.W. and Anderson, A.F. "Axially laminated anisotropic rotors for reluctance motors", Proc. IEE 1966, 113, pp 2058-2060.

5. Park, R.H. "Two-reaction theory of synchronous machine", Trans AIEE, Vol 48, No. 2, July 1929, pp 716-730.

6. Doherty, R.E. and Nickle, C.A. "Three-phase short-circuit synchronous machine", Trans AIEE, Vol 49, No. 2, April 1930, pp 700.

7. Lawrenson, P.J. and Agu, L.A. "Theory and performance of polyphase reluctance machine", Proc. IEE, August 1964, 111, pp 1435-1445.

8. Silvester, P. and Chari, M.V.K. "Finite-element solution of saturable magnetic field problems", to be published.

9. Slemon, G.R. "Magnetoelectric devices", Wiley, 1965.

10. Mathur, R.M. "The starting performance of segmental-rotor reluctance machine", Doctorate thesis, Leeds University Press, 1968.

11. Prescott, J.C. and El-Kharashi, A.K. "A method of measuring self-inductances applicable to large electrical machine", Proc. IEE, Vol 106A, April 1959, pp 169-173.

12. Chalmers, B.J. and Dodgson, R. "Saturated leakage reactances of cage induction motors", Proc. IEE, Vol 116, No. 8, Aug 1969, pp 1395-1404.

13. Honsinger, V.B. "The inductance L_d and L_q of reluctance machines", Trans, IEEE Pas paper 70tP 193 PWR.

14. Alger, P.L. "The nature of polyphase inductance machine", New York, Wiley, 1951.

15. Menzies, R.W. "Theory and operation of reluctance motors with magnetically anisotropic rotors; Part I Analysis", to be published in IEEE Trans, Vol PAS.